INVESTIGATION OF THE PERFORMANCES OF CERAMIC MICRO/ULTRAFILTRATION MEMBRANES IN STABLE OIL IN WATER EMULSION PURIFICATION

A Thesis Submitted to
the Graduate School of Engineering and Sciences of
İzmir Institute of Technology
in Partial Fulfillment of the Requirements for the Degree of

MASTER OF SCIENCE

in Chemical Engineering

by
Pınar ÇETİN

March 2018
İZMİR

We approve the thesis of **Pınar ÇETİN**

Examining Committee Members:

Prof. Dr. Muhsin ÇİFTÇİOĞLU
Department of Chemical Engineering, İzmir Institute of Technology

Assist. Prof. Dr. Ayben TOP
Department of Chemical Engineering, İzmir Institute of Technology

Assist. Prof. Dr. Nilay GİZLİ
Department of Chemical Engineering, Ege University

26 March 2018

Prof. Dr. Muhsin ÇİFTÇİOĞLU
Supervisor, Department of Chemical Engineering
İzmir Institute of Technology

Prof. Dr. Erol ŞEKER
Head of the Department of Chemical Engineering

Prof. Dr. Aysun SOFUOĞLU
Dean of the Graduate School of Engineering and Sciences

ACKNOWLEDGEMENTS

It is a genuine pleasure to express my immeasurable appreciation and deepest gratitude to Dr. Muhsin ÇİFTÇİOĞLU for his precious guidance and support, understanding and encouragements throughout my graduate education and in the preparation of this thesis and also for the productive environment that he built in his laboratories.

I would like to express my gratitude to Burcu ALP and Rukiye ÇİFTÇİOĞLU for the useful comments and engagement through the learning process of this master thesis.

My appreciation extends to my colleagues and friends; Kaan YALTRIK, İklima ODABAŞI, Safiye YALDIZ, Neslihan KUTLU, Başak BAŞKARANFİLCİ, Elif YILBAŞI and Deniz ANGI for their support and encouragement during these years.

Moreover, I am greatly indebted to Zeki Selim AKBAŞ for his love.

Above all, I am most grateful to my dear family Vedat ÇETİN, Kamile ÇETİN, Göksel ÇETİN and Fatma ÇETİN for their eternal support, never ending love and encouragement during all my educational life.

ABSTRACT

INVESTIGATION OF THE PERFORMANCES OF CERAMIC MICRO/ULTRAFILTRATION MEMBRANES IN STABLE OIL IN WATER EMULSION PURIFICATION

Increasing water scarcity is an important threat to the whole world. The use of too much water during the production processes and the insufficient level of reuse of this water and the increasing quantities of oil containing waste generated in many industrial activities cause dangerous consequences for the environment. Highly concentrated oil-in-water emulsions are very harmful for aquatic life, soil, atmosphere and human health. Traditional treatment methods are not effective in the removal of emulsified oil droplets which have less than 20 μm of droplet size. Ceramic micro/ultrafiltration membranes have been explored and developed in recent years due to their superior advantages in oil containing water treatment/purification.

The aim of this MSc study was to produce tubular ceramic micro/ultrafiltration membranes for the removal of oil from stable oil in water emulsions. The prepared emulsions with about 5-6 μm of droplet sizes were fed to the crossflow filtration system and the effects of experimental parameters such as transmembrane pressure (TMP), crossflow velocity (CFV) and temperature on membrane performance/permeate flux was investigated. Titania, zirconia and neodymium doped polymeric sols were prepared and coated on the MF layer in order to investigate coating/surface modification on probable permeate flux enhancement and separation ability of the membrane. The reduction of the total suspended solid (TSS) and turbidity were determined as 100 %. A stable permeate flux with a lower extent of membrane fouling and concentration polarization was obtained with 1 m/s of CFV and 2 bar of TMP.

ÖZET

SERAMİK MİKRO/ULTRAFİLTRASYON MEMBRANLARININ KARARLI YAĞ-SU EMÜLSİYON ARITIMINDAKİ PERFORMANSLARININ ARAŞTIRILMASI

Artan su kıtlığı tüm dünya için büyük bir tehlike haline gelmektedir. Özellikle birçok endüstriyel faaliyetlerde, üretim işlemleri sırasında çok fazla su kullanılması, bu suyun yeniden kullanılmaması ve yağ içeren atıklar içermesi çevre için tehlikeli sonuçlar doğurmaktadır. Metal, gıda ve içecek, tekstil ve çelik endüstrileri tarafından üretilen yüksek konsantrasyonlu su içerisinde yağ emülsiyonları yeryüzündeki su kaynaklarının normal oksijen transfer mekanizmasını değiştirdiği için su yaşantısı, toprak, hava ve insan sağlığı için çok zararlıdır. Yerçekimi, yüzeyden sıyırma, flotasyon ve koagulasyon gibi geleneksel arıtma yöntemleri damlacık boyutunun 20 μm'den az olan emülsiyon haline getirilmiş dağ damlacıklarını uzaklaştırmak için etkili değildir. Seramik mikro/ultrafiltrasyon membranları yağ içeren sudaki üstün avantajları nedeniyle son yıllarda araştırılmış ve geliştirilmiştir.

Bu yüksek lisans çalışmasının amacı sudan kararlı yağ-su emülsiyonlarını uzaklaştırmak için seramik mikro/ultrafiltrasyon membranlarının üretilmesidir. Tübülar seramik destekler, mikrofiltrasyon (MF) katmanları elde etmek için α-Al_2O_3 sollerle kaplandı. Ultrafiltrasyon (UF) solleri böhmit tozuyla hazırlandı ve MF membranlar üzerine kaplandı. 5-6 μm yağ damlacıklarından oluşan emülsiyon yüksek süzüntü hızı elde etmek için transmembran basıncı, çapraz akış hızı ve sıcaklık gibi deneysel parametrelerin değiştirilerek incelenmesi için çapraz akışlı filtrasyon sistemine beslendi. Zarın seçici özelliğini değiştirmeden süzüntü hızını artırmak için titania, zirkonya ve neodmiyum katkılı polimerik soller hazırlandı ve MF tabakası üzerine kaplandı. Toplam askıda katı madde (AKM) ve bulanıklık 100% oranında azaltıldı. 1 m/s çapraz akış hızı ve 2 bar tansmembran basıncı membran tıkanıklığı ve konsantrasyon polarizasyonunun az olmasını sağlayarak yüksek ve kararlı süzüntü akısı elde etmeyi sağladı. Yüksek ve kararlı süzüntü akısı elde etmek için en uygun sıcaklık aralığı 35-40 °C olarak bulundu.

TABLE OF CONTENTS

LIST OF FIGURES

Figure **Page**

LIST OF TABLES

Table **Page**

CHAPTER 1

INTRODUCTION

The fresh water demand of humanity has been dramatically increasing because of the increasing world population (Eslamian 2016). Climate change, ineffective use of existing water resources and insufficient level of water reuse in industry however is creating a significant threat for humankind. The recycling of used water will be a vital issue for the environment due to the present very high levels of oil containing wastewater generated especially in the metal, food and textile industries. Wastewaters with about $2x10^4$ mg/l and $1.4x10^4$ mg/l oil contents are produced in metal and food industries, respectively (Coca, Gutiérrez, and Benito 2011).

Metal and food industries in Turkey used $7.55x10^8$ and $1.32x10^8$ m^3 of water annually and reused 47% and 26% of wastewater in their processes, respectively. Non-recycled wastewater is however a serious problem to the environment if no treatment is applied because of its high oil content. Organic compounds such as hydrocarbons, nitrogen sulphur oxygen, aliphatic and aromatic compounds and fatty acids (Padaki et al. 2015, Cheryan and Rajagopalan 1998) are present in oily water. These organic compounds change normal oxygen transfer mechanism of water and destroy the food chain from beginning to the end by affecting the algea which constitute the basic primary step of that vital chain. Oil containing wastewater pollutes not only drinking and ground water resources but also the atmosphere and the soil (Yu, Han, and He 2013b, Padaki et al. 2015). Discharge criteria are applied all around the world in order to protect the environment and it is forbidden to discharge wastewater with an oil content of above 10-15 mg/l without any treatment.

There are companies involved in the collection of oily wastewater from industries generating oil containing wastewater in their processes. The off-site treatment by these collection companies are usually not cost-effective considering the high amounts of oily wastewater. Companies usually install and run their own wastewater treatment units based on their wastewater stream characteristics as cost effective solutions (Križan Milić et al. 2013).

Traditional treatment methods such as gravity and skimming, flotation and coagulation are very common to remove free oil which has droplet sizes above 150 μm. Traditional treatment methods are cost-effective and easy to handle but they can be harmful to the environment due to sludge formation. The working principle of traditional methods mostly are based on density differences which commonly necessitates the use of chemical additives for increasing the density difference between the oil and water phases (Cheryan and Rajagopalan 1998).

Membrane technology is now commonly accepted to be the best available and promising technology for oil containing wastewater treatment. Oil can be emulsified and made soluble in water with the addition of surfactants. These emulsified and soluble oils are very stable and have smaller oil droplets which are less than 20 μm. Membrane technology has superior advantages such as being highly automated, small foot print, low operational cost and high efficiencies for the removal of these stable oil droplets from wastewater streams. The absence of the use of chemical additives in membrane treatment prevents the sludge formation problems encountered in conventional treatments (Cheryan and Rajagopalan 1998). Inorganic membranes such as ceramic membranes are the most preferred treatment methods in recent years because they can also be operated at high temperatures and pressures. Ceramic membranes are durable for a wide pH range (Hsieh 1996b, Buekenhoudt 2008). Membrane technology has many excellent features but it also has some limitations such as membrane fouling and concentration polarization which makes membrane cleaning a very important issue for a long life cycle of the membrane. Cleaning procedures of ceramic membranes are simpler than polymeric membranes because ceramic membranes are durable to the organic solvents and chemicals. Ceramic membranes with high mechanical, thermal and chemical stabilities are produced in the form of porous asymmetric multilayer structures in order to obtain high permeate fluxes with desired selectivities (Burggraaf 1996, Tsuru 2008, Hsieh 1996b).

Microfiltration and ultrafiltration ceramic membranes are effective in the removal of smaller oil droplets from water streams (Abadi et al. 2011, Lee et al. 2002). The most important operational parameters such as cross flow velocity (CFV), transmembrane pressure (TMP), temperature and pH of the feed solution are usually controlled in order to attain high permeate fluxes and oil removal efficiencies. Concentration polarization and membrane fouling are the most important limitations for micro and ultrafiltration ceramic membrane performance. Nano-coating modification for increasing the hydrophilicity of the microfiltration membrane surfaces have been investigated in recent

years towards preventing membrane fouling in addition to the research conducted on the effects of operational parameters. Nano sized γ-Al_2O_3, ZrO_2 and TiO_2 coatings have been developed to reduce the interactions between oil droplets and the membrane surface by increasing hydrophilicity of the membrane surface (Chang et al. 2010, Zhou et al. 2010, Chang et al. 2014).

The aim of this MSc study was the investigation of the development of ceramic microfiltration(MF)/ultrafiltration(UF) membranes with/without surface modifications by using three nano-coatings (pure titania, zirconia and neodmiyum doped titania of the MF membranes) and the determination of their oil retention abilities in the treatment of stable oil in water emulsions. The droplet sizes of the stable emulsions prepared by using Tween-80 surfactant and edible oil were determined by using Zetasizer DLS particle size distributions and optical microscope images. Crossflow filtration system was used for the determination of filtration performances of ceramic membranes. Effects of operational parameters such as CFV, TMP and temperature were explored in order to enhance membrane performances. Turbidity and total suspended solids of the permeates were measured by spectrophotometer in order to determine the oil retention abilities of the ceramic membranes.

This chapter is followed by Chapters 2, 3 and 4 where brief reviews on oil containing water, emulsions and traditional treatment methods are conducted, respectively. General information, basic classification and history of the inorganic membranes are included in Chapter 5. Recent research on oily wastewater/emulsion treatment by using microfiltration, ultrafiltration and modified microfiltration membranes are summarized in Chapter 6. Preparation of ceramic membranes with their selective layers, emulsion preparation and characterization and the results of this MSc study are explained in Chapters 7 and 8. The important conclusions of this work is stated in Chapter 9.

CHAPTER 2

OIL CONTAINING WATER

Developments and expanding production activities in industries such as petrochemical, metal, textile and food industries consequently increases the oily wastewater generation annually (Yu, Han, and He 2013b, Gupta et al. 2017). These industries, their sources, nature of the oil and their oil concentrations are given in Tables 2.1. and 2.2. Wastewaters with high oil contents are generated in metal industry during metal processing and finishing, hot and cold rolling, aluminum rolling and can production. Metal working fluids (MWFs) are commonly used as cooling and lubrication agents to enhance life cycle of tools especially in cutting and rolling processes. High amounts of oily wastewater with high oil concentrations are produced during these processes. Food industry is the other major industry which produces highly concentrated oily wastewater. Wastewaters with 500-14000 mg/l oil contents are produced during food processing (Coca, Gutiérrez, and Benito 2011). Palm oil production for example generates wastewaters with 4000 mg/l oil content. The wastewaters generated by these processes with high oil contents have relatively high biochemical oxygen demand (BOD) and chemical oxygen demand (COD) values (Kajitvichyanukul, Hung, and Wang 2011).

Over 37500 m^3 liquid waste was produced from over 7000 plants daily in USA and high amount of wastewater was reused in industry with primary and secondary treatment but remaining liquid waste included high concentrations of pollutants such as oil and grease (Cheryan and Rajagopalan 1998). Annual vegetable oil production was about 21.83 metric tonnes in Europe generating a very large amount of hazardous oily waste along the process (Šereš et al. 2016). Metal and food industries annually used $7.55x10^8$ and $1.32x10^8$ m^3 of water in Turkey however only 47 and 26 % of water were reused in these industries, respectively. The high oil contents of the non-recycled water make the treatment a very vital issue for the environment due to the presence of organic compounds in oily water. Oily water can contain organic compounds such as aliphatics, aromatics, nitrogen sulphur oxygen (NSO) and asphaltene and some of these hydrocarbons, phenolic compounds, surfactants and fatty acids in the oily sludge are very harmful for the environment (Padaki et al. 2015, Cheryan and Rajagopalan 1998).

Table 2.1. Sources of oily wastes from industries.
(Source: Yu et al., 2013)

Source	Industries	Nature
Alkaline and acid cleaners	Metal fabrication, iron and steel, metal finishing, industrial laundries	Normally highly emulsified due to surfactants; difficult to treat
Floor washes	All industries	Mixture of various types of oils from spills of hydraulic and cutting fluids, oil mists from spraying/coating etc.; Can be present in both free and emulsified forms stabilized by dirt and debris, and solvents
Machine coolants	Metals manufacturing, machining	Normally emulsified and difficult to treat
Vegetable and animal fats splitting, refining, rendering	Edible oil, detergent manufacture, fish processing, textile (wood scouring), leather (hide processing), tank car washing	Both free and emulsified oil; difficulty of treatment varies
Petroleum oils	Petroleum refining, petroleum drilling	Both free and emulsified oil; difficulty of treatment varies

Small amounts of oily water can be very harmful for the environment. Oily wastewater discharge above the set limits affect the groundwater resources. Drinking water resources and aquatic life both can therefore be seriously damaged because normal transfer mechanism of oxygen in water changes with the disposal of oily wastewater. Dissolved oxygen content vital for food chain changes drastically when oily water containing various concentrated contaminants is discharged. Algae is a significant initiator in the food chain and high levels of dissolved oxygen changes growth behaviour of algae since 2 mg/l of oxygen is very critical to maintain the aquatic life cycle. The

increasing level of oxygen in water however causes a higher consumption rate of oxygen by algae and other microorganisms. The food chain is consequently affected and aquatic life is destroyed because living conditions of anaerobic creatures totally change because of shift in equilibrium balance. Water pollution which is caused by releasing oily wastewater also affects crop production. The oily wastewater covers the soil in time which becomes an oily sludge clogging the pores of the soil. This harmful oily sludge can be absorbed in the pores present in soil. The plants growing in these soils can no longer grow sufficiently and normally. The ground cover disappears over time, and the growing plants become unhealthy food sources for living creatures consuming these plants. Thus, the effects starting from the lowest layer of the food chain reach people. Not only water and soil pollution but also air pollution starts. The balance of the environment is completely removed (Yu, Han, and He 2013a, Padaki et al. 2015).

Table 2.2. Sources of oily effluents.
(Source: Coca et al., 2011)

Industrial Process	**Oil Concentration (mg/l)**
Petroleum refining	20-4000
Metal processing and finishing	100-20000
Aluminum rolling	5000-50000
Copper wire drawing	1000-10000
Food processing (fish and seafood)	500-14000
Edible oil refining	4000-6000
Paint manufacturing	1000-2000
Cleaning bilge water from ships	30-2000
Car washing	50-2000
Aircraft maintenance	500-1500
Leather processing (tannery effluents)	200-40000
Wool scouring	1500-12500
Wood preservation	50-1500

There are set oil content limits which are applied in different countries around the world on the discharge of excessively produced oily water due its harmful effects on the environment. Discharge criteria of oily water oil contents generally varies in the 10 to 15 mg/l range (Lu et al. 2016). 10 mg/l of discharge criteria is applied in China (Yu, Han, and He 2013b) while some other countries enforce very tight rules for oily water discharge and they approve under 5 mg/l of discharge criteria (Lu et al. 2016). Discharge criteria can be extended to 100-150 mg/l for synthetic oils (Križan Milić et al. 2013).

2.1. Types of Oil

Oily water can be classified as free (floating) oil, dispersed oil, emulsified oil and dissolved oil according to its contents. These four groups and their droplet sizes are represented in Table 2.3. Free oils are visible on water surface with higher than 150 μm of droplet diameter. Dispersed oil is stable due to electrical charge interactions/repulsions. This type of oily water is surfactant free and the oil droplet size usually is in the broad range of 20 to 150 μm. The most important difference between dispersed oil and emulsified oil is the presence of surfactants. Different types of surfactants are used to obtain stable oil in water emulsions with less than 20 μm of oil droplet diameter. Dissolved oil which has less than 5 μm of oil droplet size is chemically dispersed. Treatment methods which will be discussed in chapter four are chosen by considering oil types and their droplet sizes. Emulsified oil properties will be explained in the next chapter since recent research on emulsified oil treatment will be discussed in the following chapters in more detail.

Table 2.3. Types of oil and droplet size in oil-in-water mixtures.
(Source: Coca et al., 2011)

Type of oil	**Droplet diameter, D_p (μm)**
Free oil	≥ 150
Dispersed oil	20-150
Emulsified oil	≤ 20
Dissolved oil	≤ 5

CHAPTER 3

EMULSIFIED OIL

Emulsion appears to have a homogeneous and stable structure visually but it contains one or more immiscible liquids a heterogeneous structure. Oil droplets in such stable emulsions collide and merge to each other slowly which causes oil and water phase separation in time. The speed of this phase separation is closely related to the surfactant type/content used as an emulsifier for formation of the stable emulsion. Emulsions can be prepared by three different routes. The application of mechanical forces is the first route which is conducted through pumping and mixing processes. Surfactants/emulsifiers are added to these processes in the second route. In industrial processes surfactants are used for the preparation of stable emulsions. The last route involves heating since increased temperatures can modify some chemicals in the formation of emulsions. Microemulsions with 5-100 nm of droplet sizes are also a subgroup of emulsions and they are visually transparent (Kajitvichyanukul, Hung, and Wang 2011).

Emulsions are classified as oil-in-water (O/W) and water-in-oil (W/O) based on the continuous phase as schematically shown in Figure 3.1. The emulsion is called as O/W if water is used higher than 30 % as a continuous phase and oil is dissolved in water homogeneously. On the other hand, W/O emulsion is obtained, if water is less than 25 % and water droplets are trapped in the continuous oil phase.

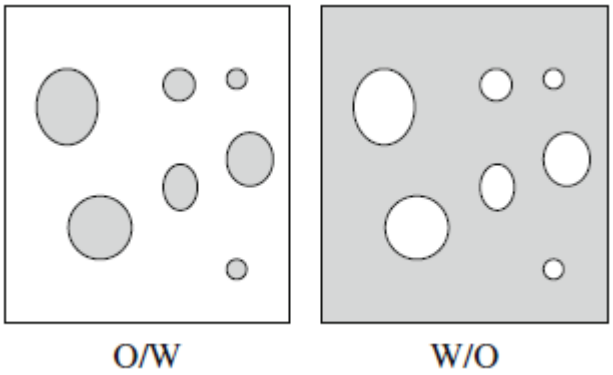

Figure 3.1. Different types of emulsions as oil droplets in water and water droplets in oil. White and gray areas represent water and oil, respectively.
(Source: Kajitvichyanukul et al., 2011)

Stability of emulsions and droplet size can be controlled by surfactants. Normally, oil and water phases separate if there is no external factor such as heat or energy. Surfactants are added to oil and water mixture to obtain a stable emulsion. These surfactants with significantly larger molecular structures decrease the surface tension of water and oil mixture upon their addition to the mixture (Nair et al. 2003). Figure 3.2. shows the structure of Tween-80 surfactant.

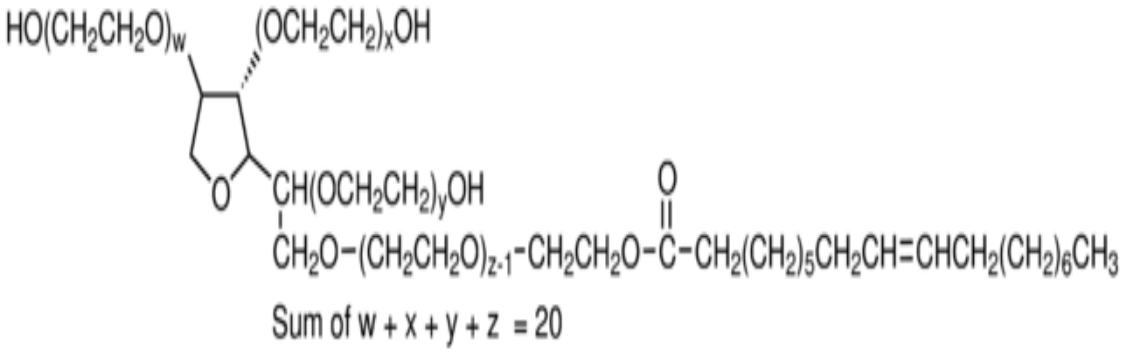

Figure 3.2. Molecular structure of Tween-80 surfactant.
(Source: Nair et al., 2003)

A surfactant consists of a hydrophilic head and a hydrophobic chain. Hydrophilic head can be either polar or ionic. The hydrophilic head and the hydrophobic chain of a surfactant is schematically shown in Figure 3.3. Hydrophilic head is water soluble. On the other hand, hydrophobic chain has weak interactions because of London dispersion force. Long hydrocarbon chain is known as hydrophobic chain of the surfactant. Surfactants are classified as anionic, cationic, amphoteric and non-ionic with respect to the hydrophilic group property. Anionic surfactant is composed of negative head whereas cationic surfactant consists of negative head as opposed to anionic surfactant. Sodium dodecyl sulfate (SDS) and cetyl trimethyl ammonium bromide (CTAB) are the most common examples of anionic and cationic surfactants, respectively. Both positive and negative charges are present in amphoteric surfactants such as cocamidopropyl betaine (CAPB). Non-ionic surfactants with no charged heads in their structure such as Tween-80 are commonly used in the preparation of emulsions.

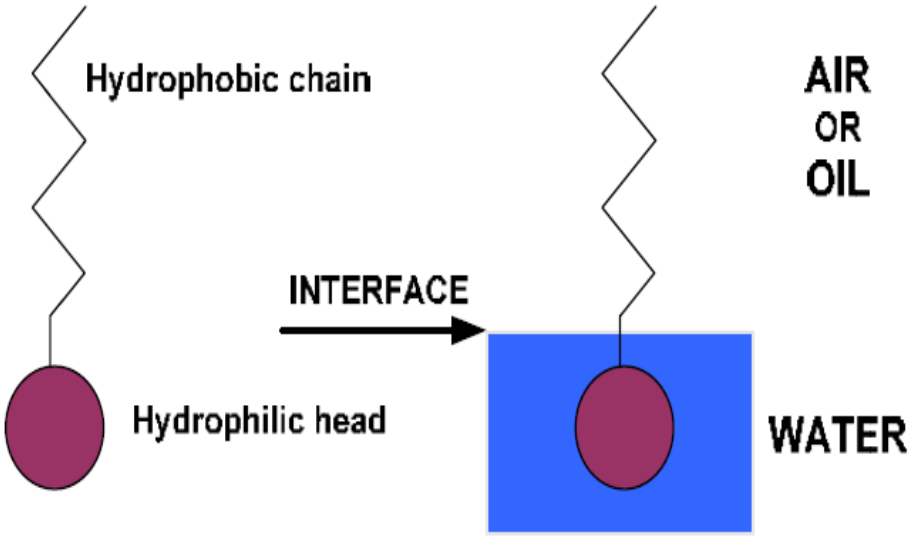

Figure 3.3. Molecular structure of a surfactant and its orientation at the interface. (Source: Coca et al., 2011)

Critical micelle concentration (CMC) is one of the most important properties of the emulsions because above CMC surface tension remains constant. Surfactant molecules have no association tendency and hence no orientation below CMC. O/W and W/O surfactants above CMC that form micellar structures are shown in Figure 3.4. Temperature, surfactant properties and concentration are the parameters affecting the micelle structures. Hydrophobic and hydrophilic character of the emulsion can be estimated by hydrophilic-lipophilic balance (HLB) equation;

$$HLB = \frac{20M_h}{M} \tag{3.1}$$

M_h and M represents hydrophilic mass and total mass of surfactant, respectively. HLB scale changes from 0 to 20. If HLB equals to zero, surfactant molecule has completely hydrophobic structure. On the contrary, completely hydrophilic structure is obtained when HLB equals to 20. O/W emulsions are generally prepared with HLP values in between 10 and 20 because of their hydrophilic structure (Coca, Gutiérrez, and Benito 2011).

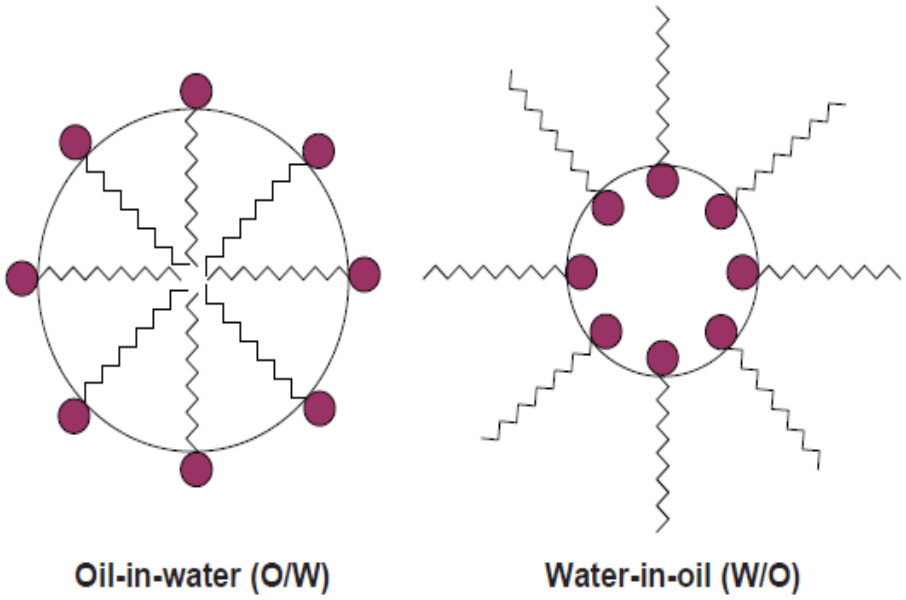

Figure 3.4. Surfactant stabilized micelles.
(Source: Coca et al., 2011)

3.1. Characteristics of O/W Emulsions

O/W emulsions can be characterized by surface and interfacial tension, contact angle, zeta potential and droplet size measurements. Surface and interfacial tension are commonly measured by du Noüy ring method. Increasing the amount of surfactant decreases surface and interfacial tension which makes the preparation of stable emulsions possible (Coca, Gutiérrez, and Benito 2011). Benito et al. (2010) investigated the use of non-ionic, anionic and cationic surfactants. Results of this study have shown that increasing the emulsifier concentration above CMC decreases the interfacial tension dramatically as shown in Table 3.1. Especially cationic surfactant has significant effect in reducing interfacial tension.

The contact angle between the solid surface and oil is an important property for the determination of wettability. The increase in contact angle (θ) causes lower wettability and non-stable emulsion formation. Lower contact angle between the oil and surface is more preferable because stable emulsions with and higher wetting surface can be prepared. Figure 3.5. represents contact angle configuration between oil-water and solid surface.

Table 3.1. Effect of surfactant concentration on interfacial tension.
(Source: Benito et al., 2010)

Concentration (times CMC)	Interfacial Tension (mN/m)		
	Non-ionic	Anionic	Cationic
0.00	19.6	19.6	19.6
0.25	5.0	11.9	3.4
0.50	5.2	9.2	2.1
0.75	4.8	9.1	1.9
1.0	3.9	9.0	1.2
1.5	3.0	7.7	1.1
2.0	2.3	7.5	1.2
10	2.3	7.7	1.2

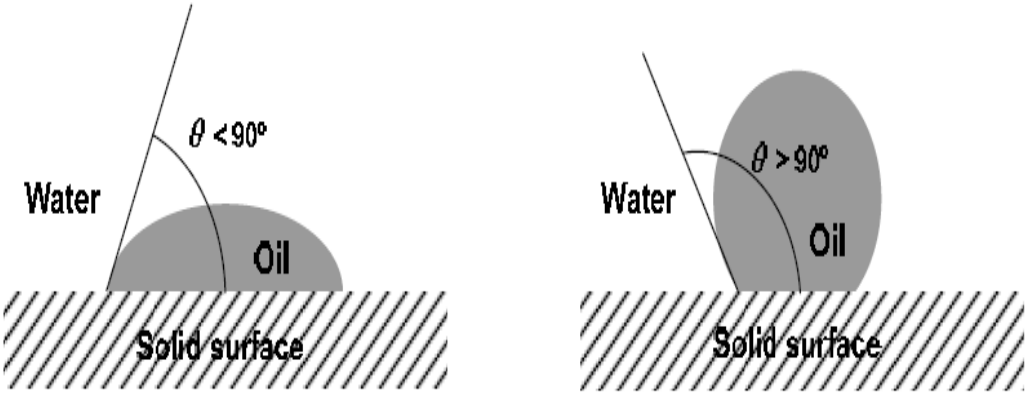

Figure 3.5. Wettability and contact angle.
(Source: Coca et al., 2011)

Stability of O/W can be correlated to zeta potential (ξ) measurements through the measurement of the velocities of emulsion droplets in a certain electrical field. Higher value of ξ regardless of whether negative or positive enhances the emulsion stability. Low interfacial tension and high stability are provided by surfactants at high zeta potential value. Droplet size distribution is an important parameter which is analyzed by microscopic techniques to select appropriate separation and treatment technique of O/W emulsions (Coca, Gutiérrez, and Benito 2011). Table 3.2. shows possible treatment technologies based on emulsion types (Benito et al. 2010).

Table 3.2. Process to remove oil from oily waters.
(Source: Benito e al., 2010)

Oily Waste	**Removal Process**
Free oil	Mechanical separations: settling, centrifugation, hydrocyclones
Emulsified oil	Membrane separations (UF, RO) Vacuum evaporations Chemical treatment (destabilization) by coagulation and flocculation Flotation Filtration/adsorption Coalescence in packed beds Deep bed filtration Electrical methods: electrocoalescence, electroflotation, electrocoagulation
Dissolved oil and additives	Vacuum evaporation Distillation Membrane reactors Biological treatments

CHAPTER 4

CONVENTIONAL TREATMENT METHODS FOR OIL CONTAINING WATER

The necessity of purification of oil containing water arises by considering the high amount and concentration of oily water and its harmful effects for the environment. There are specialized companies which receive oil containing water for offsite treatment. However, agreements with these companies are expensive because the price increases with the amount of waste. Onsite treatment methods are better than offsite treatment in terms of cost-effectiveness by considering excessive amounts of oil containing water which are produced by lots of industries (Križan Milić et al. 2013).

Treatment methods are categorized into three groups as primary, secondary and tertiary according to oil types and their stabilities as shown in Figure 4.1. Primary methods are more traditional techniques which are suitable for free oils. Secondary treatment methods are used to remove stable O/W emulsions and dispersed oil. Tertiary treatment methods are very effective to remove emulsified oils and soluble oils (Coca, Gutiérrez, and Benito 2011).

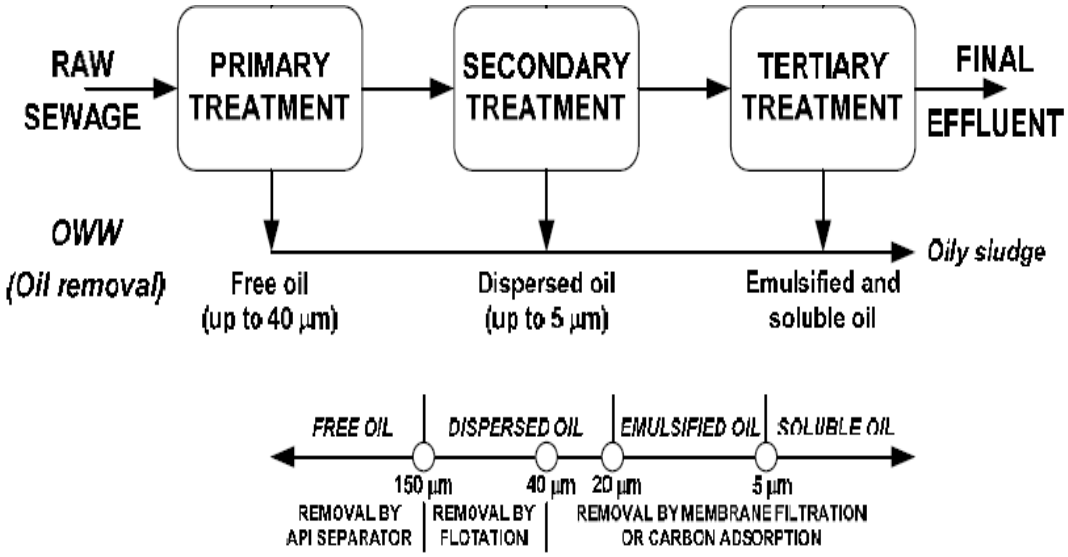

Figure 4.1. Oily wastewater treatment process according to types of oil.
(Source: Coca et al., 2011)

4.1. Primary Treatment Technology

Primary treatment technology is preferred when oil droplet size is higher than 150 µm which is called as free oil. This physical treatment technology is based on differences in density. Gravity separation is suitable for removing free oil which have higher than 150 µm droplet size. The oil on the water surface forms a layer due to density difference. This layer is skimmed from the water. API (American Petroleum Institute) separator which consists of solid separation part at the bottom and oil skimming part on the water surface is commonly used as a gravity separation method. Schematic diagram of API separator is shown in Figure 4.2. Efficiency of API separator is directly related to viscosity, density and concentration of oil, amount of surfactant and stability of oil contaminated water, droplet size of oil and flowrate. API separation is a cost effective method for the removal of solid particles and free oil droplets. It can be also used in primary treatment technology (Coca, Gutiérrez, and Benito 2011, Cheryan and Rajagopalan 1998).

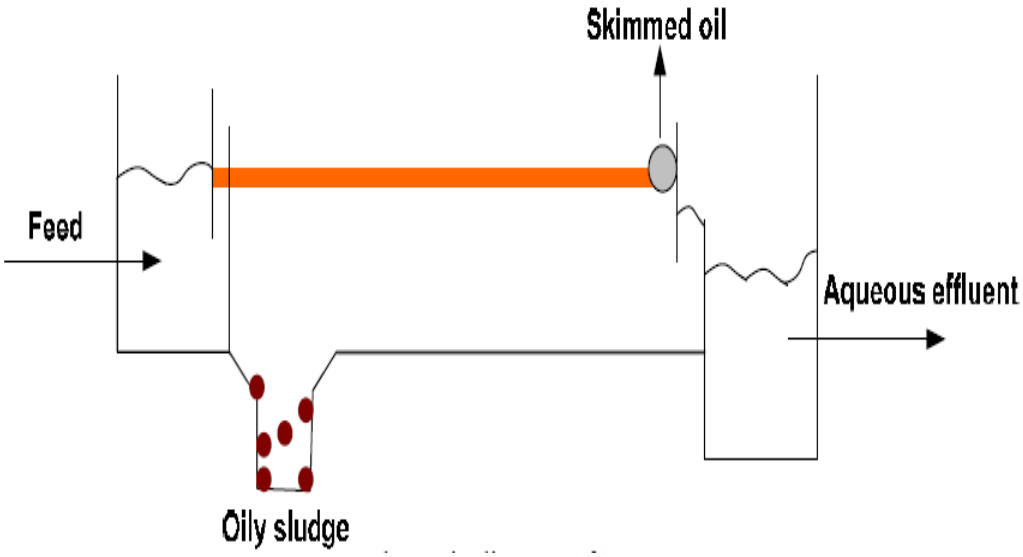

Figure 4.2. Schematic diagram of API separator.
(Source: Coca et al., 2011)

Centrifugal separation equipment such as centrifuges and hydrocyclones can be used in primary separation method. Centrifugal separation is a transition method before coagulation. Centrifugation is a more effective method than gravity based separation in

terms of time efficiency and small foot print. While oil containing water flows from a circular rotating device, water which is heavier than oil passes from the circular region to outer region with the centrifugal force and oil is removed from the vortex region. The working principle of hydrocyclone is based on circular motion. Feed which is composed of oil and water is fed to the hydrocyclone system as shown in Figure 4.3. Water is collected from the bottom because it is the heavier phase and oil is removed from the top of the hydrocyclone unit. Hydrocyclones are commonly used in metalworking industry because of high efficiency and low capital cost to remove the oil and solids.

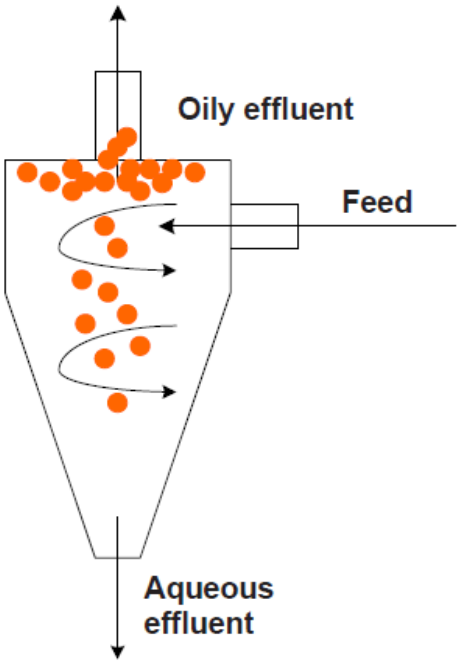

Figure 4.3. Schematic diagram of a hydrocyclone
(Source: Coca et al., 2011).

4.2. Secondary Treatment Technology

Secondary treatment methods are used to remove oil from O/W emulsions and dispersed oil with chemical, physical and electrical methods. Coagulation and flocculation are chemical treatment methods due to the addition of chemicals to the oil contaminated water. Coagulation is accomplished by coagulants which aid in forming larger oil droplets which can be removed by gravity settling. Chemical coagulants such as $AlCl_3$, $FeCl_3$, $CaCl_2$ and $FeSO_4$ are used to destabilize O/W emulsions. Adding these

coagulants decrease the zeta potential and increase the interfacial interaction between oil and water (Coca, Gutiérrez, and Benito 2011). The oil removal efficiency varies with the coagulant type and chemical properties. Coagulation based treatment methods however cause sludge formation and undesired secondary pollution (Yu, Han, and He 2013b).

Flotation is a physico-chemical method to remove emulsified oil. Relatively small density differences between oil and water phases is increased by the attachment of fine air bubbles. Air bubbles attach to the surface of the oil droplets as shown in Figure 4.4. Air bubbles and oil droplets agglomerate and rise upwards which makes their removal from the water phase significantly easier. The most common flotation type is dissolved air flotation (DAF) which involves the use of compressed air. Compressed air dissolves in oil contaminated water under pressure. Flotation causes the formation of a certain density difference between water and oil rich phases. Air is further removed in flotation tank by decreasing pressure after the separation process. High removal efficiencies can be obtained by dissolved air flotation but this separation method may become inadequate for treatment due to the problems related with chemical addition, sludge formation and high operating costs (Križan Milić et al. 2013).

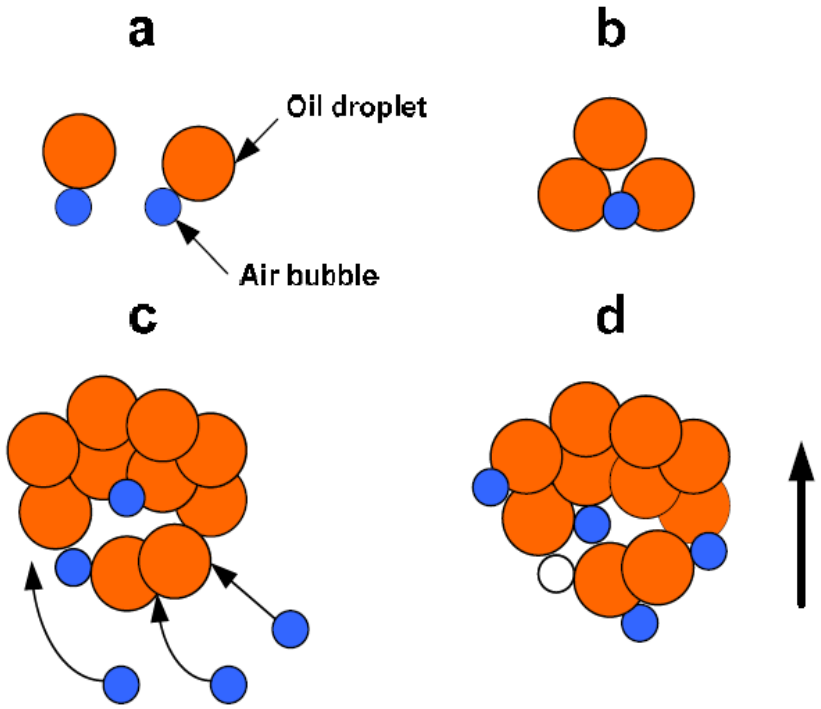

Figure 4.4. Interaction mechanism between gas bubbles and oil droplets during flotation. (Source Coca et al., 2011)

Traditional methods such as gravity, flotation and coagulation are very effective for oil removal from wastewater streams with low cost and they are easy to handle. However, there are some limitations of traditional methods. Chemical agents must generally be used to enhance the density difference between oil and water rich phases which generates sludge formation problems. Traditional methods are not sufficiently automated and require well-trained operators. Corrosion problems may occur because of acidification. Traditional methods may be inadequate in satisfying the discharge criteria in the treatment of oil containing water when the high amounts of oily water produced by many industries are also taken into consideration (Cheryan and Rajagopalan 1998). Membrane technology can therefore be used for the removal of oil from oily wastewater as a secondary treatment method due to its superior advantages. High efficiency is provided by membrane technology with low operational cost. There is no need to chemical addition during the treatment which prevents sludge formation. Highly automated membrane technology has small foot print area.

4.3. Tertiary Treatment Technology

Tertiary treatment technology is suitable for soluble waste oil. Tertiary treatment methods such as evaporation, activated carbon adsorption and biological treatment are generally not preferred for oil containing wastewater. The water discharge criteria can be met by membrane separation based treatments. Evaporation is commonly used for small amounts of waste because evaporation necessitates high levels of energy where the liquid waste is heated for the evaporation of the volatile liquid. Oil contaminated waste is removed after evaporation. Evaporation is conducted by mass transfer. Water rises to the upward of the liquid sample. Thin layer is formed by repulsive forces of the oil droplets as in Figure 4.5. Water transports from this thin layer with mass transfer. Thin water layer is formed and water transforms to the vapor phase. Evaporation rate change with stability of O/W and type of the surfactant. Evaporation method is not sufficient without any other treatment method because it decreases volume of the waste but oil contaminants are not totally removed. Disposal cost can be decreased by evaporation.

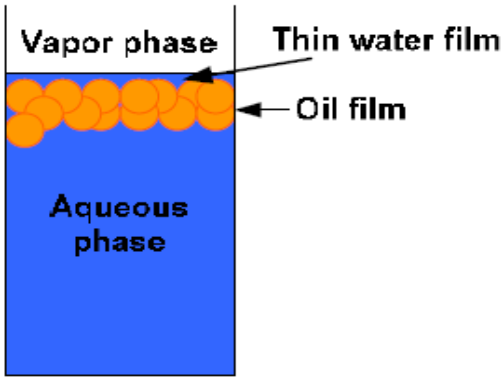

Figure 4.5. Schematic process of evaporation.
(Source: Coca et al., 2011)

Activated carbon adsorption is the final stage after primary and secondary treatment. Remaining organic compounds after the secondary treatment are removed by adsorption. Adsorption modification is preferred to increase efficiency (Coca, Gutiérrez, and Benito 2011). Biological treatment is conducted by microorganisms. It is a very useful method for obtaining high COD and TOC removal efficiency with low cost. However, it is very difficult process in terms of operation because temperature and pH directly affect microorganism efficiency. Microorganisms can die at high temperature or low pH (Yu, Han, and He 2013b, Coca, Gutiérrez, and Benito 2011). Table 4.1. summarizes some of the treatment processes for oil removal from oily wastewater along with their advantages and disadvantages.

Table 4.1. Advantages and Disadvantages of Oily Wastewater Treatments.
(Source: Milic, 2013)

Treatment	**Advantages**	**Disadvantages**
Gravity separation and skimming	Effective for removing free oil and suspended particles Low cost	Not effective in removing smaller oil droplets and emulsions
Dissolved air flotation (DAF)	High oil removal efficiency	High investment and operation costs Difficult in terms of operation Sludge problem and chemical needed

(Cont. on next page)

Table 4.1. Cont.

Treatment	Advantages	Disadvantages
Chemical coagulation and flocculation	Low cost and availability of coagulants Natural coagulants Easy to handle	Corrosion problem Low efficiency Corrosion Recontamination Hazardous activated sludge
Coalescence	No chemical additives Simple device requirement Low investment cost Long operation cycle High removal efficiency	Low efficiency due to emulsifier Decrease in coalescence lifetime Poisoning and loss of effectiveness
Adsorption	No chemical additives Low capital cost High COD removal efficiency	Cannot be used for high oil and emulsifier concentrations Difficult in terms of operation Regeneration of spent absorbent
Biological Process	Low investment costs and operating costs	Difficult in terms of operation Inhibition of the biological activities Slow process
Membrane Filtration	No chemical additives Low investment and operational costs Rarely difficult in terms of operation Small space occupancy High COD removal efficiency and oil removal efficiency	Required backwashing Fouling problem

CHAPTER 5

INORGANIC MEMBRANES

Semipermeable membrane separation is an important and highly preferred technology which allows the passage of desired components with a certain driving force such as pressure, charge or concentration (Hsieh 1996b). The most important factors for membrane system applications are their lower energy requirements, small foot print, easy operation and the use of considerably lower additional chemicals (Rijn 2004). Membranes can be classified as polymeric or inorganic. Polymeric membranes are commonly used in many areas but thermal and pH resistance of polymeric membranes are not as high as inorganic membranes. The most important membrane materials, their separation applications and operating conditions are summarized in Table 5.1. Inorganic membranes can be operated at high temperatures and have a high chemical resistance at high and low pH (Hsieh 1996b, Buekenhoudt 2008). Unlike polymeric membranes, inorganic membranes are durable to organic solvents and other chemicals which makes cleaning processes much easier. In addition to the thermal and pH stability of inorganic membranes, mechanical strength is very high (Hsieh 1996b). Inorganic membranes can be used at high transmembrane pressures. High permeation rates can be achieved with multi-layer inorganic membranes and molecular cut of levels can be adjusted through thin selective layer structure control (Levanen 2004). These very important advantages of inorganic membranes have attracted an important level of research interest on these materials in the last couple of decades.

5.1. History of Inorganic Membrane

Membrane technology has come into prominence in the recent years and extensive R&D on membrane technology is currently conducted globally. The investigations on membranes and the relevant transport phenomena started in the 18th century and these studies continue until up today (Lee 2013). Technological developments were initiated by Thomas Graham with dense metal membranes especially palladium (Hsieh 1996a). The technological developments up to 2000s are listed in Table 5.2. Commercially

porous membrane filters were discovered by Zsigmondy in the beginning of 1900s and used in microbiology. Microporous porcelain and Vycor-type glass membranes were developed in 1940s. Porous silver membranes were commercially used in 1960s in small sizes/areas.

Table 5.1. Commonly used membrane materials and their properties.
(Source: Hsieh, 1996)

Material	**Application(s)**	**Approximate maximum working temperature (ºC)**	**pH range**
Cellulose acetates	RO, UF, MF	50	3-7
Aromatic polyamides	RO, UF	60-80	3-11
Fluorocarbon	RO, UF, MF	130-150	1-14
Polyimides	RO, UF	40	2-8
Polysulfone	UF, MF	80-100	1-13
Nylons	UF, MF	150-180	
Polycarbonate	UF, MF	60-70	
Polyvinyl chloride		120-140	
PVDF	UF	130-150	1-13
Polyphosphazene		175-200	
Alumina (gamma)	UF	300	5-8
Alumina (alpha)	MF	>900	0-14
Glass	RO, UF	700	1-9
Zirconia	UF, MF	400	1-14
Zirconia (hydrous)	DM (RO, UF)	80-90	4-11
Silver	MF	370	1-14
Stainless steel (316)	MF	>400	4-11

The first large scale application started with gaseous diffusion in 1940s to produce nuclear weapons by enriching uranium. Fissionable uranium ^{235}U and non-fissionable Uranium ^{238}U isotopes constitute uranium with weight percent of 0.72 and 99 %, respectively. Uranium structure is completed with trace amount of ^{234}U. The minimum ^{235}U requirement for producing nuclear weapons is 90% and gaseous diffusion is one of

the most effective method for the enrichment of ^{235}U. Composite membranes were developed in France in order to increase mechanical strength and permeability of thin layer with increasing thickness of the selective thin layer. Porous inorganic membrane developments were sustained by US, Soviet Union, China, England and Sweden. However, gas centrifuging and atomic vapor laser isotope were developed to enrich uranium instead of porous membrane separation and these recent technologies caused a competition. Membrane technology was recognized for liquid phase microfiltration and ultrafiltration during the uranium enrichment process at the end of 1970s. In the next studies, zirconium hydroxide and polyacrylic acid mixture was precipitated on porous support in order to obtain stronger dynamic membranes. These dynamic membranes consisted of metal oxides and were developed by Union Carbide to use in large scale applications such as eliminating of contaminant from pulp and paper industry and removing of polyvinyl alcohol in textile industry. Oily wastewater treatment with membrane technology began in 1973 (Salahi, Abbasi, and Mohammadi 2010).

Table 5.2. The historical milestones of membrane technological development (pre 2000s). (Source: Lee, 2013).

Year	**Development/Discovery**	**Scientist(s)**
1748	Discovery of osmosis phenomenon	A. Nollet
1833	The law of gaseous diffusion	T. Graham
1855	Phenomenological laws of diffusion	A. Fick
1860-1880s	Semipermeable membranes:osmotic pressure	M. Traube, W. Pfeffer, J.W. Gibbs, J.H. van't Hoff
1907-1920	Porous membrane filters	R. Zsigmondy
1920s	Research on reverse osmosis	L. Michaelis, E. Manegod, J.W. McBain
1930s	Electrodialysis membranes	T. Teorell, K.H. Meyer, J.F. Sievers

(Cont. on next page)

Table 5.2. Cont.

Year	Development/Discovery	Scientist(s)
1950s	Electrodialysis, micro- and ultra-filtration, hemodialysis and ion-exchange membranes	Many
1963	Defect-free, high flux, asymmetric reverse osmosis membranes	S. Loeb, S. Sourirajan
1968	Spiral wound RO membranes	J. Westmorland
1977	Thin film composite membranes	J. Cadotte
1970-1980	Membrane and process improvements	Many
1980s	Industrial membrane gas separation process	J.M.S. Henis, M.K. Tripodi
1990s	Hybrid and novel membrane processes	Many

5.2. Classification of Inorganic Membranes

Inorganic membranes can be classified according to operation mode, size, driving force and structural characteristics. Driving force can be pressure, concentration and voltage but pressure driven inorganic membranes are generally used in filtration processes. Table 5.3. gives a summary of inorganic membrane classification (Hsieh 1996b).

Table 5.3. Inorganic membrane classification.
(Source: Hsieh, 1996)

Separation Type	Separation Process
Driving force	Pressure, concentration, voltage
Operation mode	Dead-end filtration, crossflow filtration
Structure	Dense, Porous
Size	Microfiltration, ultrafiltration, nanofiltration, reverse osmosis

5.2.1. Operation Mode Base Classification

Operation mode is classified as dead-end and crossflow filtration based on feed stream direction. Feed and permeate streams flow perpendicular to the perm-selective membrane in dead-end while the feed flows parallel to the membrane surface in cross-flow filtration. Cross-flow filtration is commonly used because membrane can be protected from concentration polarization and fouling by preventing accumulation so dead-end filtration is limited to laboratory R&D work (Hsieh 1996b).

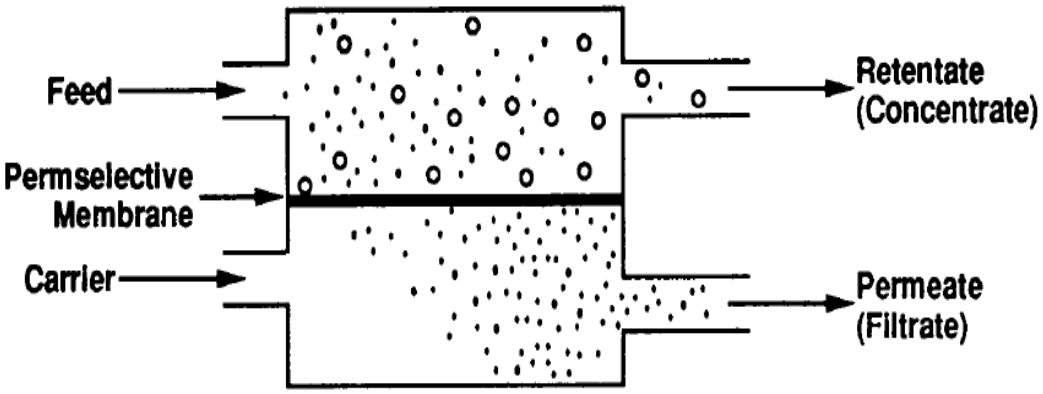

Figure 5.1. Schematic diagram of a crossflow filtration mode.
(Source: Hsieh, 1996)

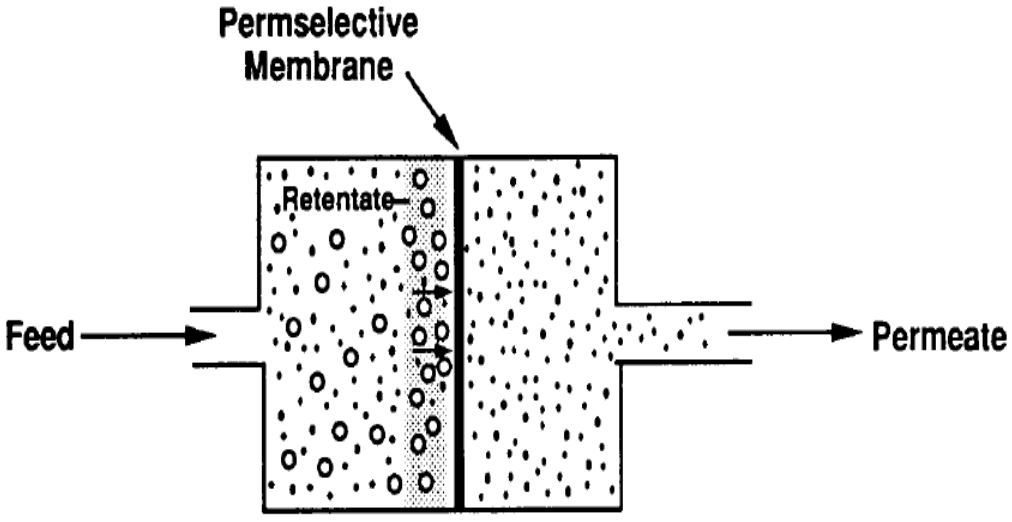

Figure 5.2. Schematic diagram of a dead-end filtration mode.
(Source: Hsieh, 1996)

5.2.2. Structural Based Classification

Membranes can be produced with dense or porous structures. The separation mechanisms of these membranes are schematically shown in Figure 5.3. Dense membranes are also known as nonporous membranes and mass transport is achieved through diffusion. Driving force of diffusion can be pressure or concentration. Diffusivity and solubility of one of the components present in a mixture in the membrane determine the transport rate of that diffusing species (Baker 2012). There are no pores and voids in dense membranes. Separation ability of the dense membrane is directly related to the membrane material and diffusivity of components through this membrane (Hsieh 1996b). Metal films are generally used with palladium support for hydrogen and oxygen separation. Permeation of hydrogen occurs through the thin metal membrane by diffusion (Levanen 2004, Tsuru 2008).

Porous membranes are composed of metal, oxide or glass porous top layer and porous support which is generally produced from metal-oxides. Porous membrane can be produced from ceramic materials such as alumina, zirconia or titania with single wall or multilayered structure (Burggraaf 1996). These metal oxide selective layers can be prepared by sol-gel techniques. Separation efficiency of the porous membrane is determined by the pore size distribution and nanoscale pore sizes in the 1 nm to 50 nm range can be obtained by sol-gel techniques and they are very vital in determining affinity, permeability and adsorption ability (Tsuru 2008).

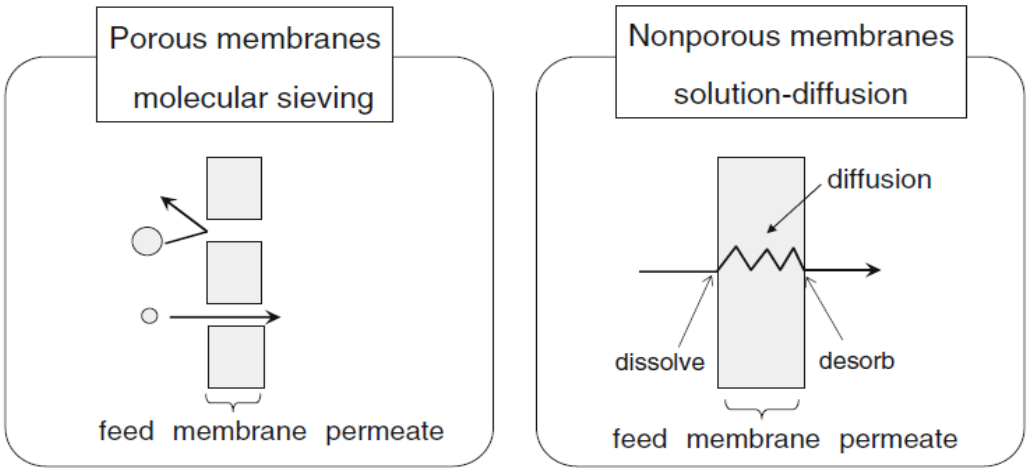

Figure 5.3. Separation mechanism of porous and nonporous membranes. (Source: Tsuru, 2008)

Inorganic membranes can be produced in symmetric or asymmetric structures. Symmetric membrane is also called as isotropic membrane and exhibits a homogeneous distribution throughout the membrane with higher mechanical strength as shown in Figure 5.4. Membrane thickness design have a determining effect on permeate flowrate. Membrane is mechanically strong if the thickness is too much, but at the same time flow rate is low. Mechanical strength becomes lower if the thickness is reduced in order to increase flow through the thin layer (Hsieh 1996b).

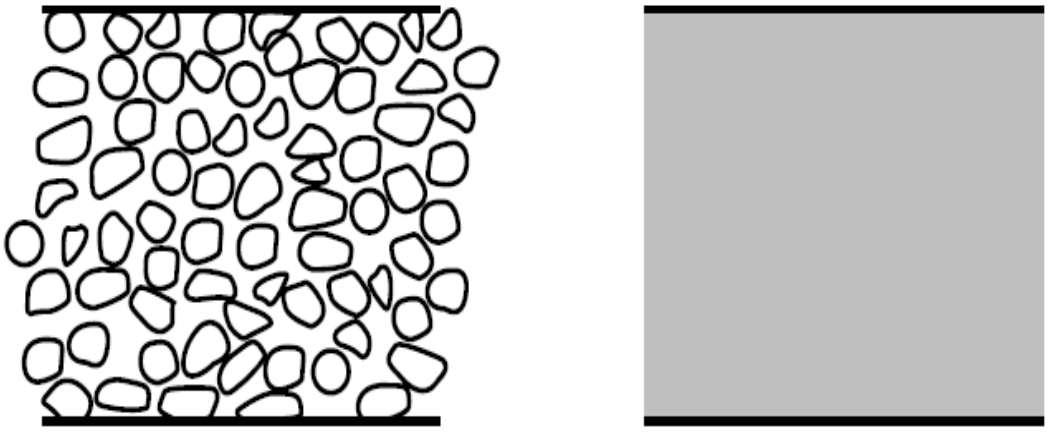

Figure 5.4. Schematic diagram of porous and nonporous symmetric membranes. (Source: Baker, 2012)

Asymmetric membrane structures are appropriate solutions for obtaining higher fluxes through thin layers possessing desired selectivities. Asymmetric membranes are formed from a number of layers with gradually decreasing pore sizes. An SEM photo of an inorganic asymmetric membrane structure is given in Figure 5.5. Support layer has a larger pore size and provides high mechanical strength. Support is generally produced by extrusion or slip casting method from alumina (Al_2O_3), titania (TiO_2) and zirconia (ZrO_2) powders. Support layer mainly provides a strong surface for the following considerably thin selective layers. Intermediate layers are formed before the top layer for gradually reducing the pore sizes. Intermediate layers are prepared by sol-gel methods with desired pore sizes and applied on support layer by dip coating technique. Thin layer which has the tightest selective capacity is coated on intermediate layer. Drying and thermal treatment is applied in order to obtain stable and strong membrane layer structures. Sol-gel parameters and heat treatment conditions are mainly closely controlled for designing/obtaining the desired layer pore sizes (Buekenhoudt 2008, Hsieh 1996b,

Burggraaf 1996). Asymmetric membranes are superior to symmetric membranes since they provide higher permeate fluxes and mechanically stronger structures. Asymmetric membranes are better developed and much more commonly used (Rijn 2004).

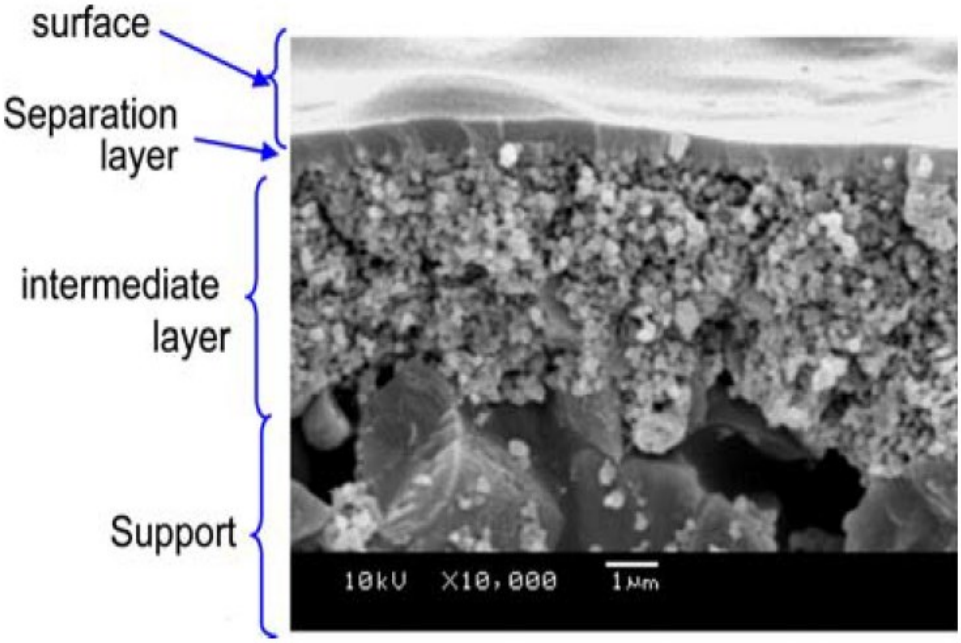

Figure 5.5. Cross-sectional SEM photo of porous ceramic membrane.
(Source: Tsuru, 2008)

5.2.3. Size Based Classification

Membranes can be classified as microfiltration (MF), ultrafiltration (UF), nanofiltration (NF) and reverse osmosis (RO) according to their pore sizes in pressure driven separations. Microfiltration membranes which have 50 nm to 5 μm pore sizes are preferred for the filtration of particles and macromolecules such as proteins. Solid particles and macromolecules are retained since they can't pass than through the pores while the solution passes through the pores (Tsuru et al. 2001, Rijn 2004). Aqueous solution containing the dissolved species is called as the permeate stream for microfiltration while suspended particles stay in the retentate stream. Microfiltration is an effective process which is widely used as pre-treatment especially in the food industry. Microfiltration has a great advantage in food industry as well as pharmaceutical, biotechnology and water treatment applications (Hsieh 1996b).

Ultrafiltration is used in food and beverage industry, pharmaceutical, biotechnology, crude oil separation from water and oily wastewater treatment applications with 5 to 50 nm pore size range. Biologicals such as viruses or dissolved substances of bacteria, colloids and macromolecules are concentrated in the retentate. Molecular weight of the retained molecular species varies in the 10000 to 500000 Dalton range. Water and salts pass through the pores and are present in the permeate stream (Hsieh 1996b, Rijn 2004). The nature of solids/molecular and ionic species present in the permeate and the retentate streams in ultrafiltration and microfiltration are schematically shown in Figure 5.6.

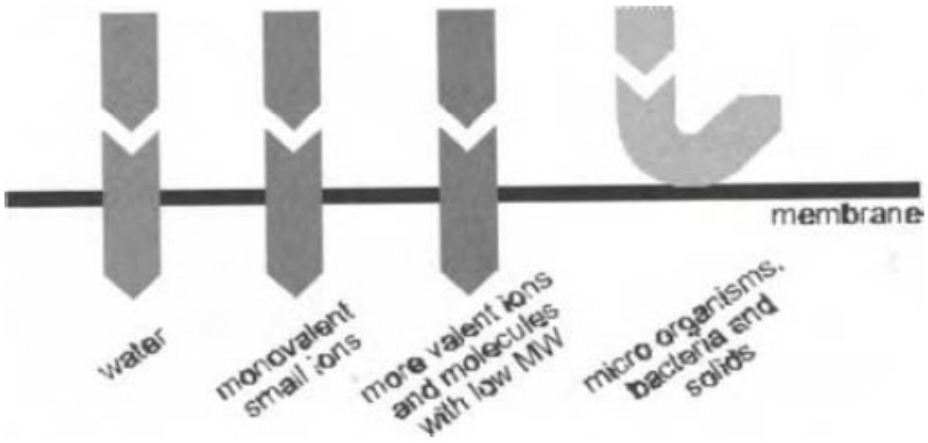

Figure 5.6. Separation processes of ultra and microfiltration membranes.
(Source: Rijn, 2004)

Eriksson is the first researcher who introduced nanofiltration term in 1988. Research on nanofiltration membrane separations which is relatively new when compared with microfiltration and ultrafiltration based separations is currently attracting significant interest. Nanofiltration membrane pore sizes lie in between ultrafiltration and reverse osmosis (1 to 10 nm) membrane pore sizes (Rijn 2004). Smaller species with about 200-20000 Dalton molecular weight are separated from solutions and are retained. Schematic representation of nanofiltration based separation is shown in Figure 5.7. Nanofiltration membranes can be titania, zirconia, silica-zirconia and γ-alumina based and are used in the separation of organic compounds and ions from aqueous solutions such as wastewater (Tsuru et al. 2001, Rijn 2004). Materials used in porous membrane structures along with their pore sizes are schematically shown in Figure 5.8. Nanofiltration is generally used in the separation of salts from dyes especially in textile industry and in acid removal from sugar.

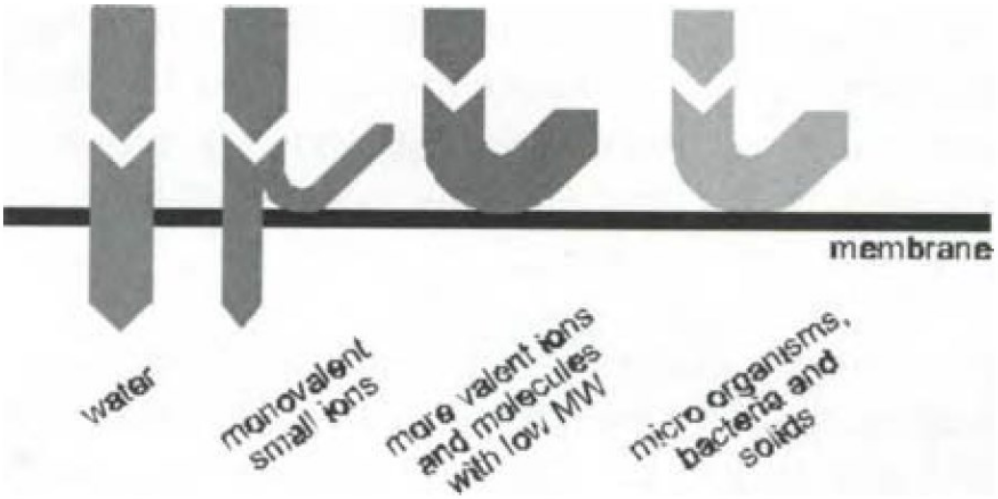

Figure 5.7. Separation processes of nanofiltration membranes.
(Source: Rijn, 2004)

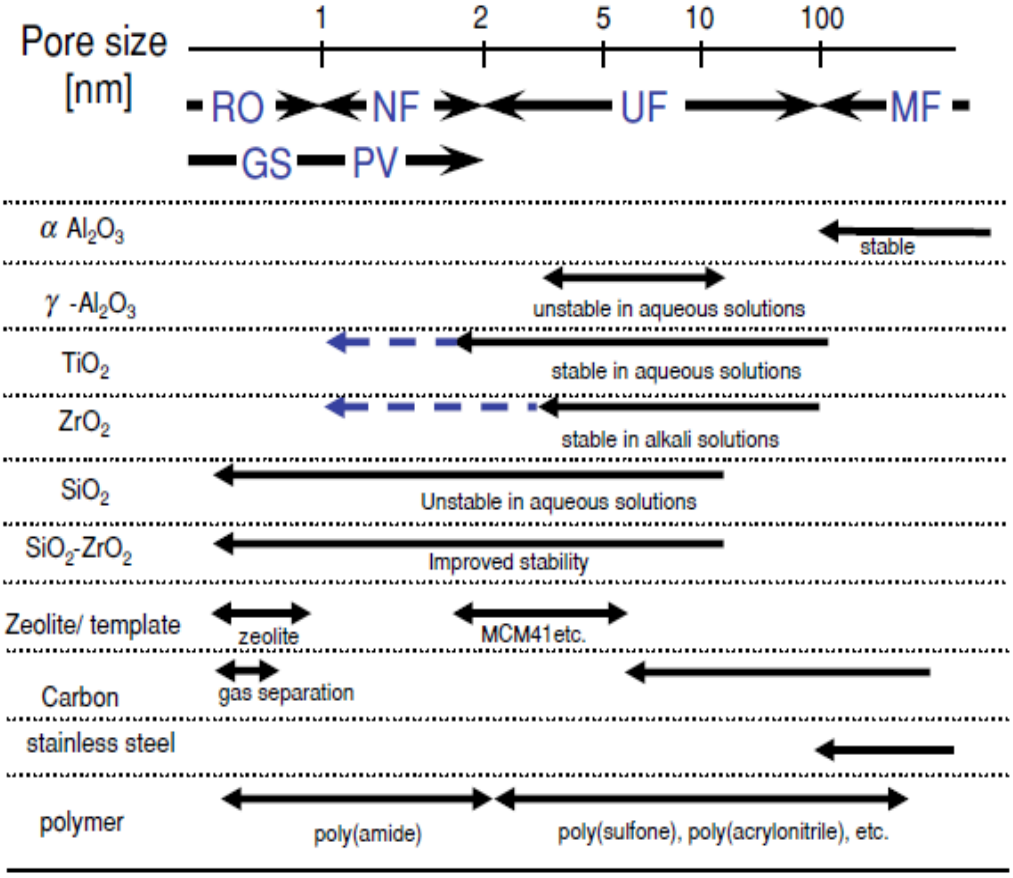

Figure 5.8. Materials and pore sizes of porous membranes.
(Source: Tsuru, 2008)

Reverse osmosis membrane pore sizes are smaller than 1 nm and they are generally used in the monovalent ion removal from solutions with high pressure driving forces (10-70 bar). Reverse osmosis can be used in desalination of seawater and in food industry. An overall summary of microfiltration, ultrafiltration, nanofiltration and reverse osmosis membrane properties and their applications is presented in Table 5.4.

Table 5.4. Filtration process types, their properties and applications.
(Source: Rijn, 2004 and Hsieh 1996)

Filtration Process	**Pore size**	**Separation Capability**	**Pressure (bar)**	**Application**
Microfiltration	50 nm-5 μm	Bacteria and colloid retention, suspended materials, protozoa	0.5-3	Prefiltration in water treatment, dye industry, food and beverage industry, screening of bacteria
Ultrafiltration	5-100 nm	Bacteria and colloid retention, macromolecules with molecular weight range: 10000-500000 Daltons	0.5-5	Dairy industry, beverage industry, pharmaceutical industry, separation of water from crude oil, separation of fruit and vegetable extracts, waste water treatment
Nanofiltration	1-10 nm	Permeation of small substances such as salt Molecular weight range: 200-20000 Daltons	5-25	Purification of sugar from acids, salts from dyes, water treatment, desalination
Reverse osmosis	<1 nm	All suspended and dissolved materials	10-70	Desalination, food and beverage

CHAPTER 6

MEMBRANE TECHNOLOGY FOR OIL CONTAINING WATER

Microfiltration and ultrafiltration studies have increased over the past years as conventional treatment methods lead to inadequate treatment technology for smaller oil droplets. Microfiltration and ultrafiltration ceramic membranes have great benefits due to less chemical additive use and lower cost than the conventional treatment methods (Abadi et al. 2011, Lee et al. 2002). MF and UF membranes are both investigated in oil-in-water treatment by using various operational parameters in order to obtain high flux because concentration polarization and membrane fouling are one of the most important limitations of these membranes. Nano-coating modified MF membranes were developed to enhance hydrophilic structure of the membrane surface without changing the separation layer. Nanosized γ-Al_2O_3, ZrO_2 and TiO_2 coatings have been studied by researchers to decrease interactions between oil droplets and membrane surfaces in recent years (Chang et al. 2010, Zhou et al. 2010, Chang et al. 2014).

6.1. Microfiltration for Oil in Water Emulsions

The effects of operating conditions on tubular ceramic microfiltration membrane performance was investigated by Lee et al. (2002). Alpha alumina support (48 % porosity and 500 bar mechanical strength) which was produced by extrusion method was coated with 1.8 μm particle size α-alumina suspension by slip casting method as an intermediate layer for MF membrane preparation. Intermediate layer was dipped into an α-alumina slurry (0.4 μm mean particle size) for 10-30 s. Three different solid contents (10, 20, 30 wt %) and dipping times (10, 20, 30 s) were investigated in order to determine the best MF thickness for high flux and crack free layer formation. Low solids content levels caused micro-crack formation while high levels resulted in a thickness of 50-60 μm with lower fluxes. The results of this work indicated that 20 wt % solids content with 20 s of dipping time were the optimum MF layer formation parameters. Figure 6.1. shows SEM images of the intermediate layer and MF which represents their thicknesses as 30 and 35

μm, respectively. Soluble waste oil which had 11 μm emulsion droplet size was filtered with this membrane at three different crossflow velocities (1, 1.5, 2 m/s) to obtain better flux and low levels of membrane fouling and concentration polarization. The results have shown that flux increases with crossflow velocity (CFV) and 135 l/m^{2}h of flux was achieved with 2 m/s of CFV.

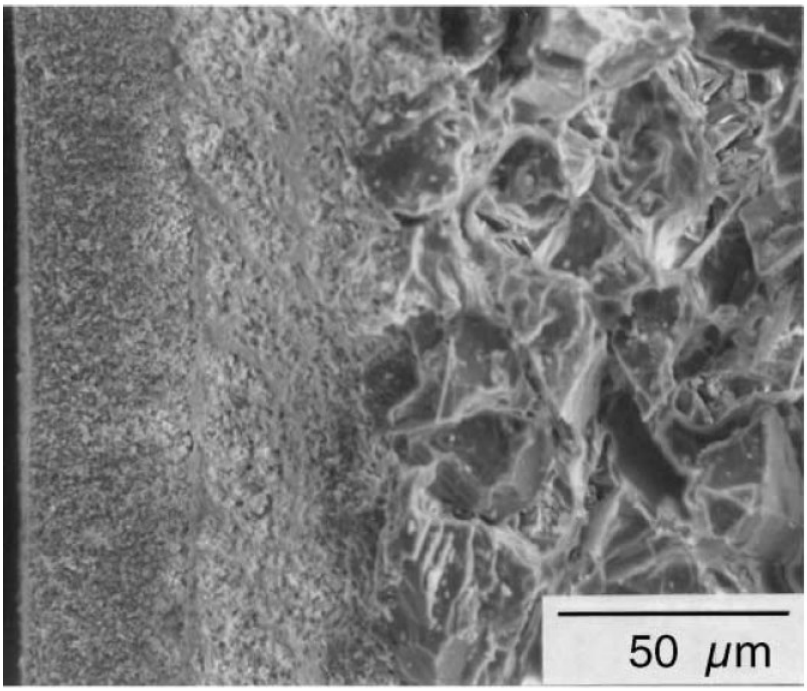

Figure 6.1. Cross section SEM micrographs of MF membrane.
(Source: Lee et al., 2012)

Abadi et al. (2011) investigated the effect operation conditions like transmembrane pressure (TMP), crossflow velocity (CFV) and temperature on permeate flux, removal efficiency of total organic carbon (TOC) and fouling behavior of tubular α-alumina ceramic membrane. α- Al_2O_3 ceramic membrane had 19 channels (OD=4 mm) and 0.2 μm pore size. The support with a porosity of higher than 33 % had about10 bar of mechanical strength. Emulsions with less than 20 μm droplet size was filtered through these membranes at 0.75-1.75 bar of TMP. Their results have shown that increasing TMP increased permeate flux up to 1.25 bar. After 1.25 bar the oil droplets clogged the pores with the effect of high TMP which caused accumulation of oil droplets on the membrane surface and concentration polarization. TOC removal efficiency decreased on the other hand at higher TMP because oil droplets started to deform and pass through the membrane pore structure along with the permeate stream. Abadi et al. determined 97.8 % TOC removal efficiency with approximately 250 l/m^{2}h flux. The results of Abadi et al.

confirmed Lee et al. because Abadi et al. studied in the 0.75-2.25 m/s CFV range and they found that increasing CFV increased the permeate flux. They stated that higher CFV caused turbulent flow and increased mass transfer coefficient close to the membrane surface which prevented concentration polarization and membrane fouling. However, after 2.25 m/s, TOC removal efficiency decreased. A natural organic layer was formed on the membrane surface causing fouling at low CFV. After 2.5 m/s this layer became very thin and some of the organic matter passed through the membrane pores and decreased TOC removal efficiency. Abadi et al. also increased the temperature from 25 to 40 ºC and they found that the observed flux increase (2-fold increase) was directly related to the increase in temperature due to lower viscosity. However, after 32.5 ºC TOC removal efficiency started to decrease with increasing operational cost. On the other hand, Abadi et al. achieved decreasing oil content, total suspended solid (TSS) and turbidity as 85, 100 and 98.6 % efficiency, respectively.

Hua et al. (2007) used tubular ceramic membrane which formed by 19 channels and total height and diameter were 425 mm and 30 mm, respectively. TMP was changed from 0.5 bar to 3 bar and 2 bar TMP was determined as optimum pressure because after this point flux and TOC removal efficiency decreased from 98.6 % to 92 % due to concentration polarization. 0.21-1.68 m/s CFV range was used to understand the effect of CFV on flux and TOC removal efficiency. Increasing CFV enhanced flux and prevented concentration polarization because of lower viscosity and higher Reynold number. Too high turbulent flow was undesirable for TOC removal efficiency. Therefore, optimum CFV was 1.68 m/s for this study. Oil concentration was the other parameter to enhance permeate flux and TOC removal efficiency. High oil concentration was not suitable for filtration because oil droplets plugged membrane surface and reduced permeate flux. However, Abadi et al. observed that TOC removal efficiency increased when oil concentration increased from 250 to 1000 mg/l. Steady flux was affected from pH of oily water. Permeate flux suddenly increased from 3.8 to 5.8 pH. However, when pH was increased from 5.8 to 9.9, flux suddenly decreased from 163 to 141 l/m^2h. Hua et al. explained that permeate flux directly related to feed property besides membrane surface property. Figure 6.2. shows the size and zeta potential of feed with changing pH value. Size of droplets did not change too much with pH but stability demonstrated some differences. Higher steady flux was achieved with higher pH because oil droplets became more negative and inter-droplet repulsion increased. Therefore, accumulation of oil droplets on the membrane surface and concentration polarization were avoided. Higher

pH was required to achieve high steady flux because TOC removal efficiency was not affected from pH while steady flux increased with pH. Hua et al. investigated the effect of salt concentration on permeate flux and TOC removal efficiency. Their results showed that higher salt concentration caused low permeate flux but their results were inconsistent with literature.

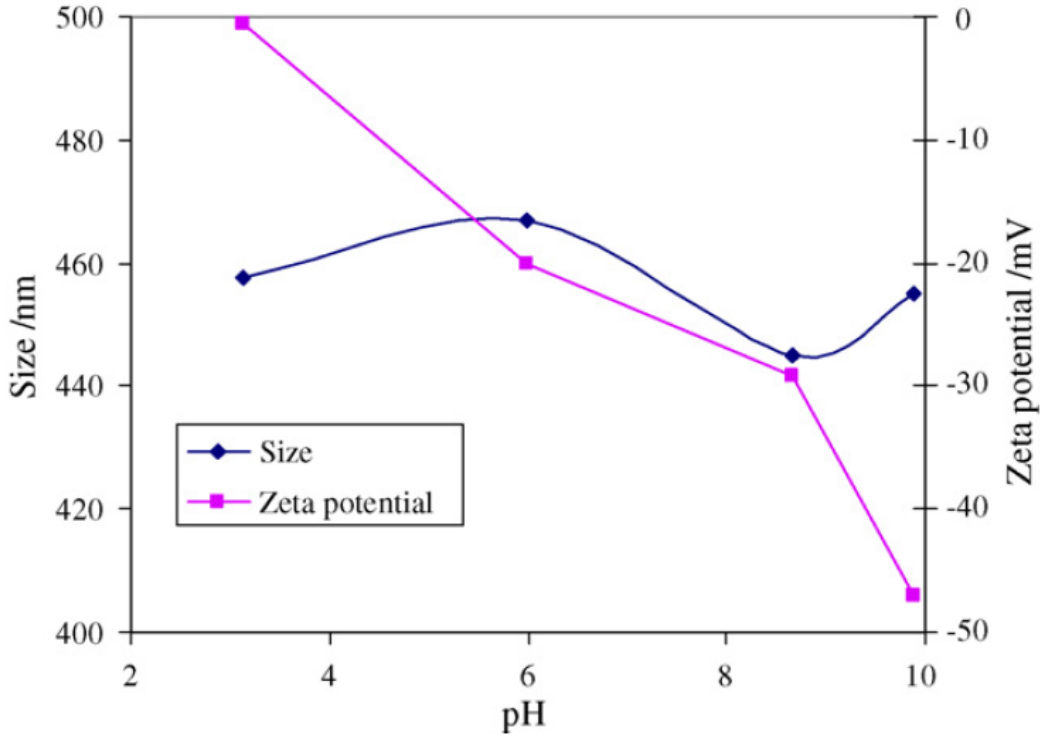

Figure 6.2. Effect of pH on size and zeta potential of emulsion droplets. (Source: Hua et al., 2007)

6.2. Ultrafiltration for Oil in Water Emulsions

Srijaroonrat et al. (1996) studied with four different types of tubular ceramic ultrafiltration membranes in terms of pore size, type of coating and hydrophilic or hydrophobic character. Table 6.1. summarizes characteristics of membranes with water. They continued their studies with backflushing and without backflushing (Srijaroonrat, Julien, and Aurelle 1999). Their studies proved that backflushing had great advantage for steady higher flux. Srijaroonrat et al. studies showed that higher transmembrane pressure enhanced flux for emulsion which was 11 µm. Flux increased from approximately 260 to 410 l/m^{2}h when pressure increased from 1 to 3 bar without backflushing. After 3 bar, flux

started to decrease. According to their studies the contact angle of the oil drop on the membrane surface ($\theta_{o/w}$), interfacial tension between oil and water ($\gamma_{o/w}$) and average pore diameter (r) were 160 °C, 33.7 dyne/cm and 0.1 μm, respectively. Calculated capillary pressure was found to be 14.16 bar. Applied pressures which were 1, 2, 3 and 4 bar were less than capillary pressure. If the applied pressure was greater than capillary pressure, membrane surface could become fouled. Deformability of oil droplets causes passing of oil from the membrane surface. Consequently, Srijaroonrat et al. did not observe any contamination and oil in permeate.

Table 6.1. Characteristics of the ceramic membranes.
(Source: Srijaroonrat et al., 1999)

Type of coating	**Pore size (nm)**	**Character**	**Permeability (l/m^{2}h)**
Hydrophobic	50	Zirconia	1042
Hydrophobic	100	Zirconia	3316
Hydrophobic	500	Alumina	5031
Hydrophilic	100	Zirconia	2200

Srijaroonrat et al. used three different CFV which were 0.47, 0.94 and 2.16 m/s in order to understand the effect of CFV on permeate flux. Their results were compatible with literature since permeate flux increased with CFV. Steady flux approached to zero when CFV was less than 0.5 m/s and permeate flux reached 400 l/ m^{2}h with 0.94 m/s CFV. Increasing permeate flux was caused by high shear rate on membrane surface at higher CFV. Oil concentration was also significant parameter on permeate flux because it was understood that higher oil concentration caused membrane fouling. Table 6.1. explained that higher pore size provided to obtain high flux. However, when emulsion was passed from four different membranes, capillary pressure increased with decreasing pore diameter. In fact that, if the pore diameter was 500 nm, capillary pressure was calculated as 2.8 bar and this values was less than applied pressure. As a result of decomposition of oil droplets caused concentration polarization on membrane surface. When the pore size of the selective layer was too large, oil droplets started to plug membrane pore. Srijaroonrat et al. investigated the effect of hydrophobic and hydrophilic character on steady flux and membrane fouling behavior. Perhaps the most important point of this study was that the hydrophilic membrane had higher flux than hydrophobic

membrane as in Figure 6.3. Since oil and hydrophobic surface have stronger adhesion force, oil droplets accumulate on hydrophobic membrane surface and concentration polarization is observed. This study showed that accumulated oil droplets were started to pass through the hydrophobic after 2 bar while hydrophilic surface was stable until 3 bar.

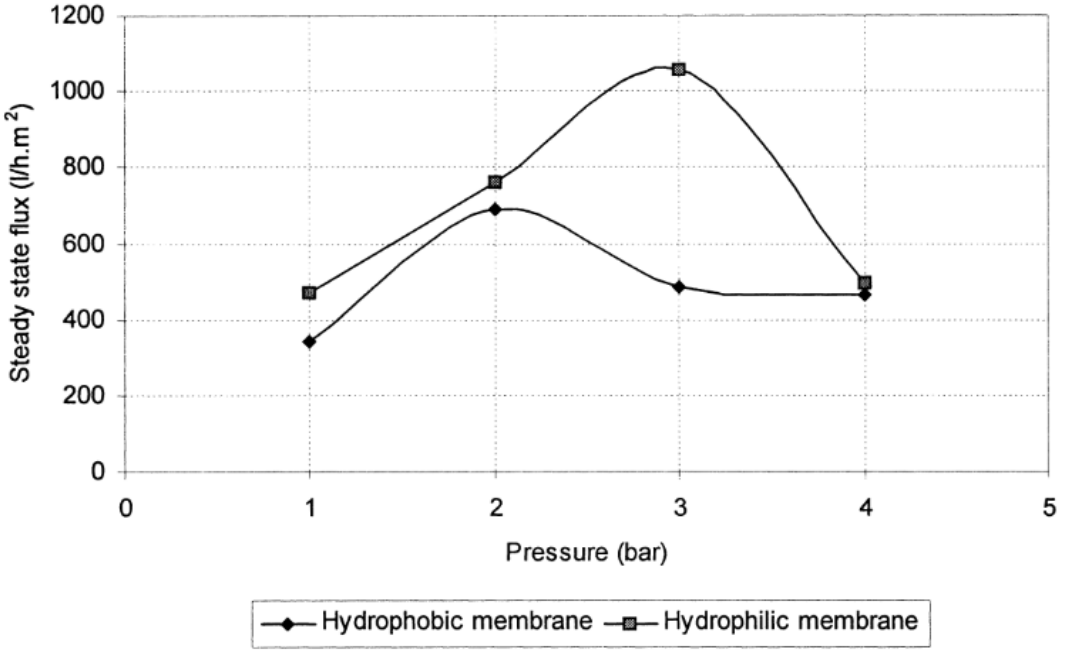

Figure 6.3. Effect of transmembrane pressure on surface modified membrane. (Source: Srijaroonrat et al., 1999)

Lobo et al. (2006) studied with tubular ceramic UF membranes which had two different molecular weight cut of (MWCO) as 50 and 300 kDa. Carbon supported ZrO_2/TiO_2 layer was used as selective UF layers. Their experiments were carried out three different CFVs (2.5, 3.4 and 4.2 m/s) under TMP range of 0.5-4 bar. Oil-in-water emulsion was prepared by anionic and non-ionic surfactant with vegetable oil in a pH range of 3-9. 3.4 m/s was chosen as optimum because flux did not change significantly after 3.4 m/s and operational cost started to increase. Permeate flux of 300 kDa UF had was higher than 50 kDa but 300 kDa had low capillary pressure due to high pore size diameter so lower CFV caused membrane fouling and concentration polarization for 300 kDa. It had been observed that COD retention did not change significantly with TMP and CFV. Isoelectric point of ZrO_2/TiO_2 ceramic membrane was 4. Membrane surface became positive charged when pH was less than pH 4. On the other hand, if the pH was higher than 4, membrane surface had negative charge. Oil in water emulsion was not affected by pH and 13.5 μm droplet size was prevented from pH. As a result, pH caused

a changes only membrane surface and adsorption mechanism. When pH value was below isoelectric point, positively charge membrane surface enhanced anionic surfactant adsorption. Therefore, positively charged membrane surface held hydrophilic tail of emulsion which was made by anionic surfactant and hydrophobic tail was held by oily water. Anionic surfactant increased adsorption with electrostatic interaction. Anionic surfactant started to pass through the membrane surface and hydrophilic surface became hydrophobic, consequently, increasing hydrophobicity decreased flux. On the other hand, if pH value was higher than isoelectric point, membrane surface became positively charged and membrane was prevented from surfactant adsorption. According to Lobo et al. results, basic pH enhanced permeate flux and COD retention.

6.3. Modified MF Membranes for Oil in Water Emulsions

Chang et al. (2010) investigated that the effect of nano sized γ-Al_2O_3 coating on ceramic microfiltration membrane with increasing hydrophilic structure. Ceramic Al_2O_3 microfiltration membranes which had 40% porosity and 0.2 μm nominal pore size were coated with aluminium isopropoxide dimethyl benzene which was prepared by 1 wt. % solution until saturation was completed. Coated membranes were washed by dimethyl benzene. XRD results of this study showed that γ-Al_2O_3 structure was achieved with small particle size of alumina grains. This alumina grains were formed by hydrolysis of aluminium isopropoxide in dimethyl benzene solution and Al_2O_3 membrane surface absorbed aluminium isopropoxide. Temperature was held at 850 °C to obtain γ-Al_2O_3. Because if the temperature is higher than 1000 °C, structure changes into boehmite. Chang et al. investigated that nano-sized γ-Al_2O_3 modification was used to change surface structure but this modification did not change inherent structures. Pore size was decreased from 0.16 μm to 0.14 μm after modification. The reduction of the pore size should have caused decreasing of the flux, but pure water flux increased from 369 to 505 l/m^2h. This could be caused by increasing of hydrophilic surface and changing contact angle of water and membrane surface. The contact angle decreases with nano γ-Al_2O_3 coating as seen in Figure 6.4. Al_2O_3 disk without nano-coating had 33 °C and the angle between water droplet and nano Al_2O_3 coated membrane decreased to 22 °C. Hydroxyl (-OH) group density increased with nano-sized modification. Consequently, membrane surface became more hydrophilic and contact angle decreased. Nano-coating Al_2O_3 modification

also increased surface roughness. On the other hand, nano-coated surface increased BET surface area and toughness. Decreasing contact angle avoided membrane surface from fouling because oil droplets started to move away from the nano-size coated surface. Although modified membrane had higher specific surface area, flux decline of modified membrane was less than unmodified membrane due to less interaction between oil droplets and membrane surface.

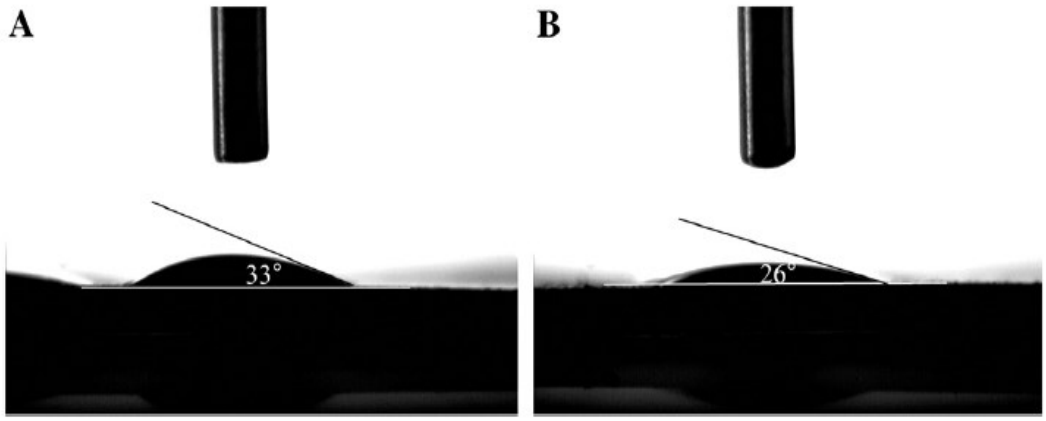

Figure 6.4. Shape of a water droplet on (A) dense Al_2O_3 disc, (B) the coating. (Source: Chang et al., 2010)

Due to high separation ability for oily water, Zirconia can be chosen as modified material. Although high cost of zirconia material causes less usage, it can be used as modified materials because of strong polar property. Zhou et al. (2010) used nano-sized ZrO_2 because of advantages of zirconia. Tubular Al_2O_3 ceramic membranes which was made of Al_2O_3 microfiltration layer, 7 channels, 40 % porosity and 0.2 µm pore diameter. The mixture of $ZrCl_4$ and absolute alcohol was used to modify Al_2O_3 membrane. Emulsion which was 1.79 µm of droplet size was prepared by engine oil, Tween 80 and Span 80. SEM images showed that nano-sized ZrO_2 coating was achieved uniformly. Nano-sized ZrO_2 coating took place on Al_2O_3 surface. Adsorption equilibrium determined the thickness of the nano-sized modified surface. Figure 6.5. shows the TEM image of ZrO_2 coating which is 100 nm of thickness. This coating increased hydroxyl group (-OH) on the membrane surface and increased hydrophilicity. On the other hand, nano-sized coating increased surface roughness as in Chang et al. study so reducing of contact angle was achieved. Flux decreased from 446 l/m^2h to 159 l/m^2h with non-modified membrane and only 33% of the flux was reversible after cleaning. On the other

hand, modified membrane had 506 l/m^{2}h at the beginning of the filtration and flux decreased to 441 l/m^{2}h. Modified membrane was cleaned easily with 88 % because removing of oil where was on the membrane surface was occurred without too much effort because of hydrophilic structure. ZrO_2 nano coating avoided sharp flux declines caused by concentration polarization and pore blocking.

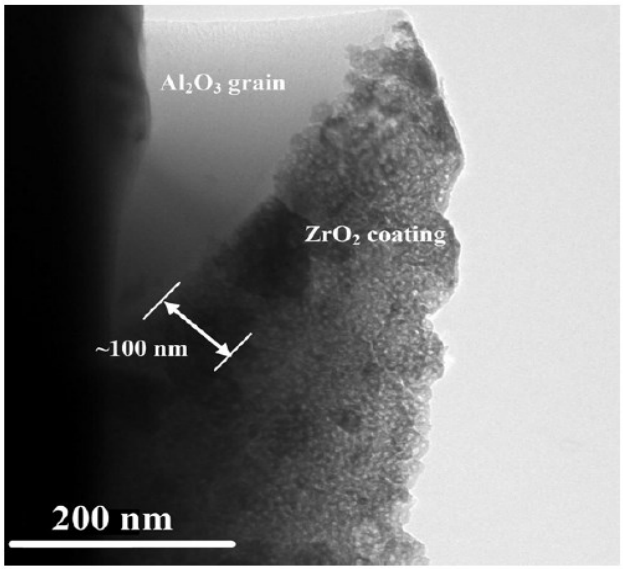

Figure 6.5. TEM image of modified Al_2O_3 grain spitted from the modified membrane. (Source: Zhou et al., 2010)

Nano-TiO_2 modification is one of the most effective coating methods for increasing hydrophilic nature of the structure and decrease contact angle between oil droplets and membrane surface. Chang et al. (2014) investigated that the effect of nano-TiO_2 modification on flux under different operational parameters such as Ti^{4+} concentration, CFV, TMP and oil concentration. Three different Ti^{4+} concentrations which were 0.1, 0.2 and 0.4 mol/l were prepared by the mixture of $Ti(SO_4)_2$ with mol ratio of $Ti(SO_4)_2$: urea as 1:2. Tubular Al_2O_3 MF membrane was saturated by the mixture and heated at 85°C to remove urea on the membrane surface and obtain TiO2. Chang et al. (2014) obtained uniform nano-coating with 30 nm without new separation layer as in Figure 6.6. Modification of MF layer provided to change surface property with reducing oil-surface interaction. This interaction was reduced by decreasing contact angle between oil droplets and surface from 33 °C to 8 °C as in Figure 6.7. Chang et al. studies in 2010, this angle was reduced to only 26 °C with nano-sized Al_2O_3 coating. This improvement

with nano-sized TiO_2 provided to achieve less interaction between oil droplets and membrane surface. Chang et al. studies showed that modified membrane with three different $Ti(SO_4)_2$ concentration had higher initial flux than unmodified membrane with 30-40 % improvement. Highest flux was achieved with 0.2 mol/l $Ti(SO_4)_2$ modified membrane because of uniform nano-sized coating. Flux of 0.3 mol/l $Ti(SO_4)_2$ modification had less than 0.2 mol/l because high concentration caused increasing thickness of modified layer, consequently, flux decreased. Membrane channels saturated with the mixture of TiO_2 and urea when the concentration of the colloidal sol was high. In addition, particle size of TiO_2 coating started to increase from nano-scale so separation layer property changed with high concentration of TiO_2.

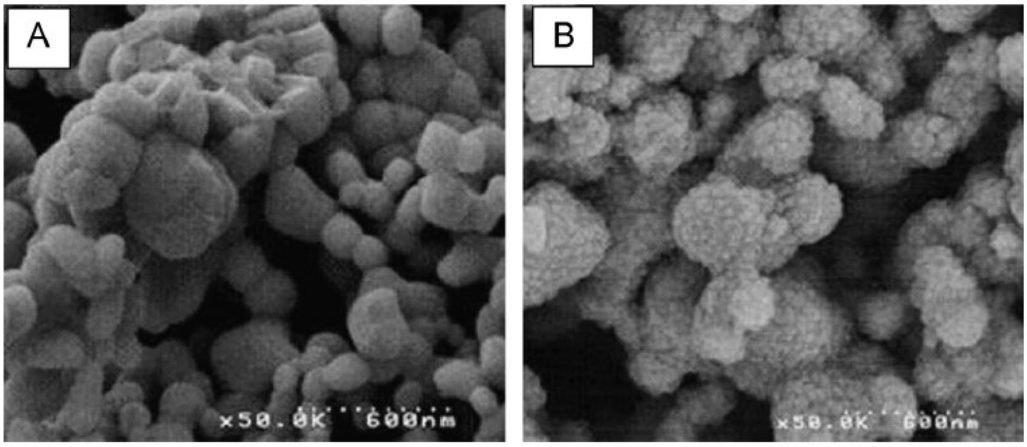

Figure 6.6. SEM images of the cross section of (A) the unmodified membrane and (B) the membrane modified with nano-TiO2. (Source: Chang et al., 2014)

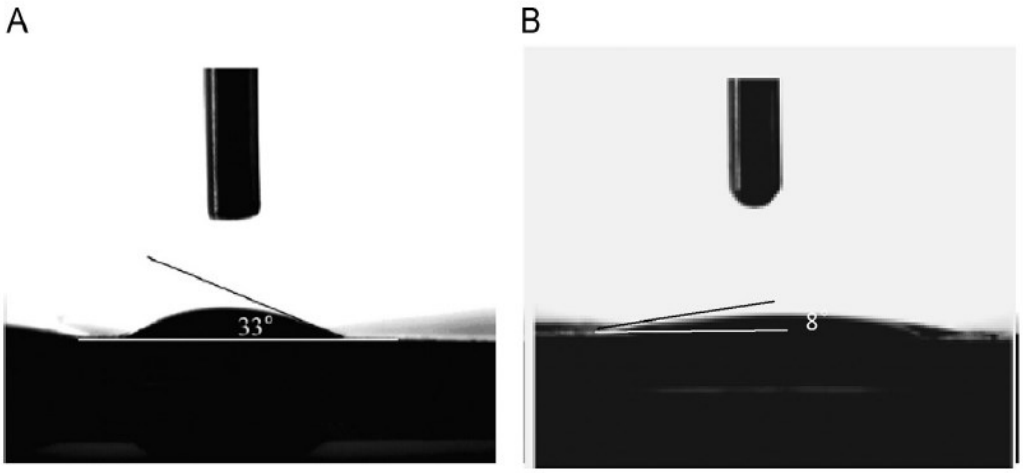

Figure 6.7. Contact angles of water on (A) dense Al_2O_3 disc and (B) nano- TiO_2 coated on dense Al_2O_3 disc. (Source: Chang et al., 2014)

Chang et al. investigated the effects of experimental parameters on permeate flux increase with 0.2 mol/l $Ti(SO_4)_2$ modified membrane. Emulsion which was prepared by hydraulic oil, Tween-80 and Span-80 with 8/1/1 weight ratio was performed through the modified membrane under 3,5 and 7 m/s of CFVs. 3 m/s caused concentration polarization. 7 m/s caused oil deformation as a result less flux. 5 m/s provided to obtain highest flux. According to Chan et al. studies deformation of oil droplets was observed. When CFV was 3 m/s, oil concentration decreased sharply but oil deformation was not observed only bigger oil droplets accumulated on the membrane surface. When CFV was increased, oil concentration decreased because cake layer formed on the membrane surface due to deformation of oil deformation. If the CVF was increased up to 7 m/s, cake layer was increased continuously and second separation layer was formed. In this study, effect of TMP was investigated that higher TMP increased flux but flux decline with time also increased because of oil droplet deformation and cake layer formation. Hydrophilic surface did not prevent the membrane from oil droplets. Temperature had significant effect on permeate flux. Increasing temperature provided high permeate flux but oil droplet deformation was observed with lower oil viscosity. Unmodified membrane tended to pore blocking at high temperature with respect to modified membrane.

CHAPTER 7

EXPERIMENTAL

7.1. Materials

Three different α-alumina (α- Al_2O_3) powders (with average particle sizes of 0.5, 1.3 and 5.2 μm), boehmite (AlO(OH)), hydroxypropyl methycellulose and glycerin were used for the preparation of tubular alumina supports. The materials used in this work is further tabulated in Table 7.1.

α-alumina powders (0.5 μm Almatis and 0.18 μm Sumitomo powders), dolapix which was used as the dispersant, polyvinyl alcohol (PVA) and defoamer were used in the preparation of stable colloidal sols used in the formation of microfiltration layers.

Two different ultrafiltration layers were prepared. The first UF layer was formed by using stable sols prepared by using disperal boehmite powder (10 nm of crystallite size and 180 m^2/g BET surface area), 65 wt.% of nitric acid and polyvinyl alcohol (PVA). P2 boehmite powder which was reported to have a 4.5 nm of crystallite size and 260 m^2/g BET surface area by the supplier were used in the preparation of the sols used for the formation of the second UF layer.

Modified MF membranes were prepared by using polymeric sols prepared from titanium (IV) isopropoxide, zirconium (IV) propoxide and neodymium (III) nitrate hexahydrate along with nitric acid, ethanol and 1-propanol.

Emulsions were prepared by using edible oil (Orkide Sunflower Seed Oil), Tween 80 as surfactant and water. Deionized water was used in the membrane and emulsion preparations.

7.2. Method

Tubular α-alumina ceramic supports were coated by MF and UF selective layers one by one to obtain asymmetric porous membrane structures. On the other hand, modified layers which were prepared by titanium (IV) isopropoxide, zirconium (IV) propoxide and neodymium (III) nitrate hexahydrate were coated on MF layers to increase

hydrophilicity. Drying and heat treatment processes were applied for all layers to obtain structures with desired thermal/chemical/mechanical stabilities.

Table 7.1. Materials used in the experiments and their properties.

Materials	**Property**
0.18 µm alumina	99.8 % purity, AKP-50, Sumitomo
0.5 µm alumina	99.8 % purity, CT 3000 SG, Almatis
1.3 µm alumina	99.8 % purity, CT 1200 SG, Almatis
5.2 µm alumina	99.8 % purity, CL 4400 FG, Almatis
Boehmite (AlO(OH))	99.8 % purity, Disperal and P2, Sasol
Hydroxypropyl methycellulose (HPMC)	Methocel F4M, The Dow Chemical Company
Glycerin ($C_3H_8O_3$)	99.5 % purity, Merck
Polyvinyl alcohol (PVA)	80 % hydrolyzed, MW= 9000-100000 g/mol, Aldrich
Dolapix CE 64	Eurokimya
Defoamer	Dağlar Kimya
Nitric Acid, HNO_3	65 %, MW=63.01 g/mol, d=1.39 g/cm^3, Merck
Titanium (IV) isopropoxide (TTIP)	97 % purity, Sigma Aldrich
Zirconium (IV) propoxide (ZTP)	70 % purity, Aldrich
Neodymium (III) nitrate hexahydrate ($Nd(NO_3)_3.6H_2O$)	99.99 % trace metal basis, Aldrich
1-Propanol	99% purity, Merck
Ethanol	99.5 % purity, Merck
Tween-80	Panreac Synthesis

7.3. Preparation of Tubular Alumina Supports

Supports with a high mechanical/chemical/thermal stability and smooth inner surfaces are important necessity for the formation of the defect free thin selective layers. Support preparation steps are schematically shown in Figure 7.1. Organic binder, three different α-alumina powders which were 0.5, 1.3 and 5.2 μm in size (in order to optimize the pore structure and mechanical properties) and inorganic binder which was boehmite were mixed in a ball mill for 2 h. These powders were kneaded by hand while adding a water/glycerin liquid mixture. Screw extruder was used to obtain a homogeneous paste and fed to the piston extruder to form the tubular ceramic supports with 16/25 mm inner/outer diameter and 200 mm in length. Extruded tubular ceramic supports were room temperature dried for a day on a roller for partial removal of water. These tubes were further dried in an oven at 90 ºC overnight. Debinding was conducted at 250-350 ºC for the removal of organics/decomposition of inorganic binder (boehmite transformation to γ-alumina) and final heat treatment was conducted at 1525ºC for 2 hours (Yılmaz 2016).

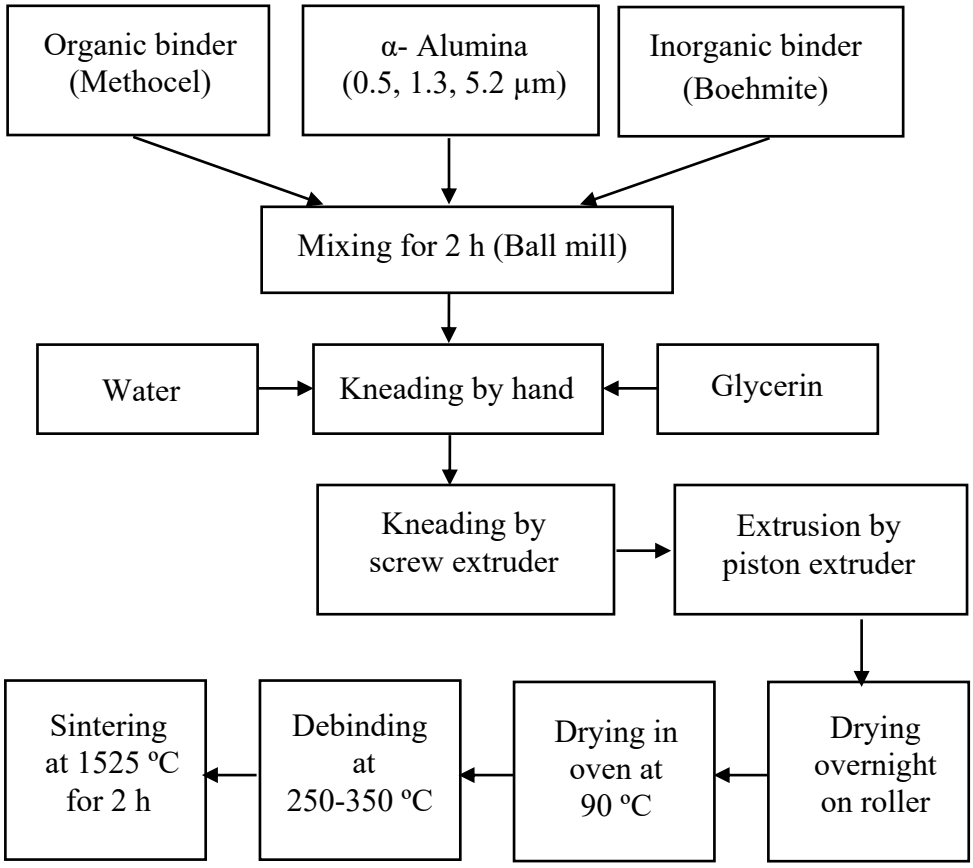

Figure 7.1. Flowchart of α- Alumina support preparation.

7.4. Preparation of MF layers

Two types of MF layers were formed by α- alumina and AKP-50 colloidal sols which had different powder particle sizes and heat treated at different temperatures. Layer processing procedure is schematically shown in Figure 7.2.

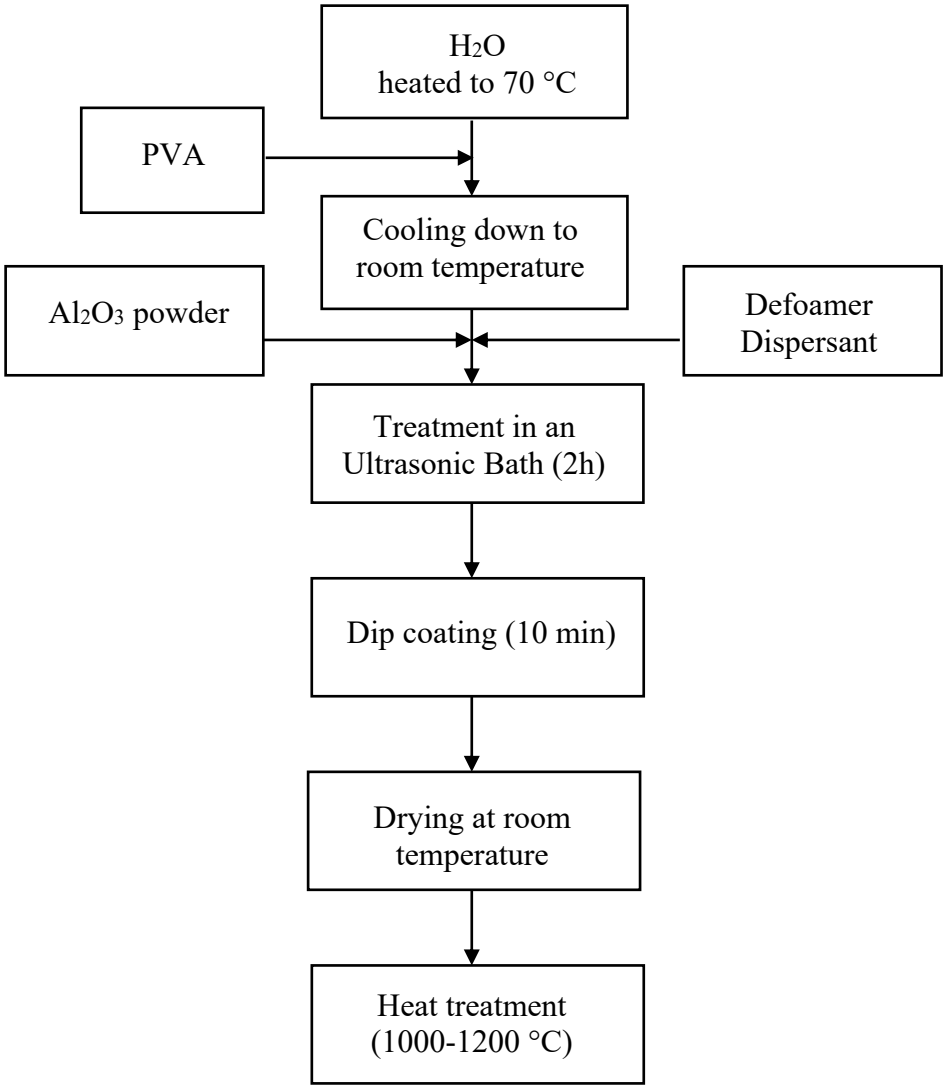

Figure 7.2. Flowchart of microfiltration membrane preparation.

PVA which was used as a binder and drying controller was added into water. Before adding PVA into distilled water, water was heated up to 70 °C in order to dissolve PVA. Mixture of distilled water and PVA was cooled down to room temperature. 7 wt. % 0.5 μm α-alumina powder was added to the cooled mixture and stirred at constant

speed. Dolapix was used as a dispersant agent to avoid agglomeration of the alumina powder. Defoamer was added to this suspension in order to minimize the presence of air bubbles during the dip coating stage. Suspension was treated in an ultrasonic bath for 2 hours in order to obtain a stable and well-dispersed colloidal sol. The suspension was kept unstirred overnight so that large particles could settle to the bottom and the suspension was collected from upper side of the bottle. The bottom of the tubular ceramic support was wrapped by a silicone rubber, filled with the stable suspension and dip coated for 10 min. A small hole was opened in the silicone rubber by using a needle where the excess of the suspension was slowly drained dropwise while creating a smooth coating surface. Microfiltration layer coated α- alumina tubes were dried vertically at room temperature for the removal of water. The MF coating was heat treated with the following schedule: furnace (Carbolite CWF 1300) was heated to 110 °C with a rate of 2 °C/min, from 110 °C to 1000 °C at 2.7 °C/min and furnace reached 1200 °C at 2 °C/min. This temperature was hold for 60 min and then cooled to room temperature. AKP-50 MF layer was prepared similarly by using 0.18 μm alumina powder and heat treated at 1000 °C instead of 1200ºC.

7.5. Preparation of Ultrafiltration Layers

Two different UF layers were prepared and used to in the oily water/emulsions treatment/purification. Preparation of the first UF layer was conducted by heating water to 70 °C similar to MF layer preparation in order to dissolve PVA (0.25 wt. %) as shown in Figure 7.3. This PVA/water solution was cooled down to room temperature and 0.8 wt. % of disperal (boehmite) powder was added into the cooled solution. 4.15 wt. % HNO_3 was added for peptization to this powder suspension while stirring at room temperature. Suspension was treated in an ultrasonic bath for the preparation of a well-dispersed sol. Tubular MF membranes were coated by UF sol by dip-coating method (similar to the above MF coating) for 10 seconds. A small hole was opened in the bottom of the silicone rubber by using a needle where the excess of the suspension was slowly drained dropwise while creating a smooth coating surface. UF coated tubes were dried at room temperature for 1 day to ensure removing most of the water from the tube body before heat treatment. The heat treatment procedure was as follows: Furnace (Carbolite CWF 1300) was heated from room temperature to 200 °C with 2 °C/min heating rate, from 200 °C to 400 °C with

1 °C/min, from 400 °C to 600 °C with a 2 °C/min heating rate. UF tubes were dwelled for 1 hour at 600 °C and then furnace cooled down to room temperature.

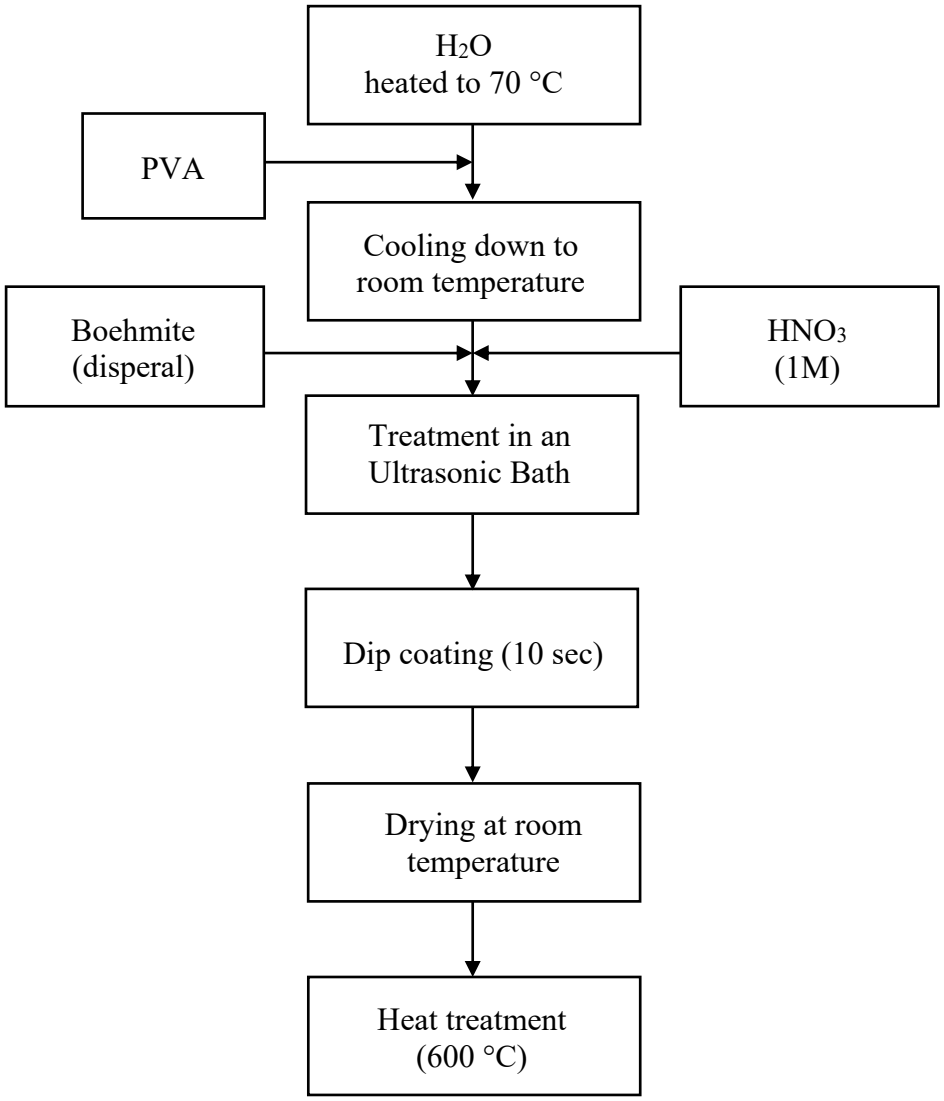

Figure 7.3. Flowchart of first ultrafiltration layer preparation.

Second UF layer (UF2) was prepared by adding 1.25 wt. % P2 boehmite powder into the stirred water. P2 boehmite sol was treated in an ultrasonic bath to obtain a uniform, stable and well-dispersed sol. Second UF layer was coated on the first UF layer (UF1) coated tube by dip-coating method like MF and UF1 for 10 seconds. UF2 coated tubes were dried at room temperature for 1 day before heat treatment process. Heat treatment was conducted at 600 °C similar to UF1 heat treatment. The UF2 layer preparation is schematically shown in Figure 7.4. An additional UF layer was also coated

on a UF2 membrane by using a sol with 0.625 wt. % P2 content with a similar procedure to the UF2 layer.

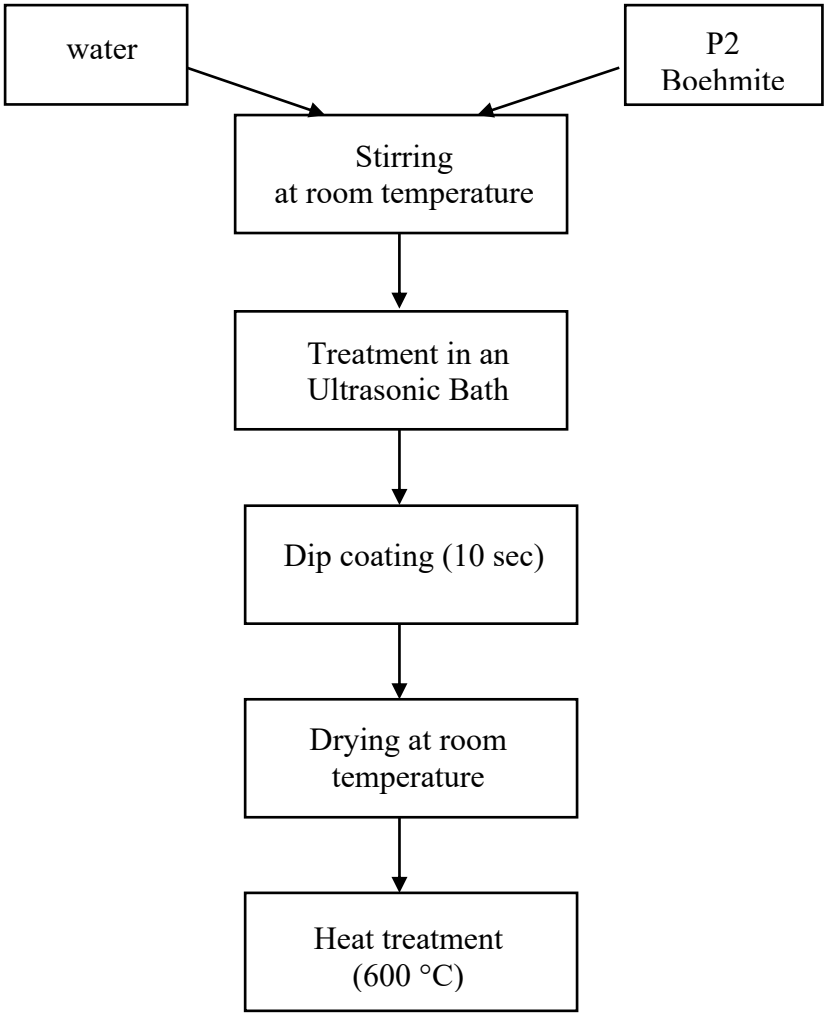

Figure 7.4. Flowchart of the second ultrafiltration layer preparation.

7.6. Preparation of Modified MF Layers

First type of modified layer was formed by using 1 wt.% pure TiO_2 polymeric sol. TTIP polymeric sol was prepared by with a 1:0.057:2:128 molar ratio of TTIP:HNO_3:H_2O:1-propanol. Alcohol-water solution and stabilized alkoxide solutions were prepared separately as shown in Figure 7.5. The controlled slow addition of TTIP was very critical for the preparation of stable alkoxide/alcohol solutions. Final polymeric sol was stirred for 90 min before coating. Tubes were coated by dip coating method for 5

minutes to saturate the tubes with the polymeric sols. Tubular membranes were dried at room temperature overnight after the coating process. Heat treatment was conducted at 300-500 °C. The second type of modified MF layer was prepared by using neodymium doped (5 wt.%) 1 wt.% polymeric TiO_2 sol. The neodymium doped polymeric sol was prepared with the same procedure followed for the pure TiO_2 polymeric sol. Neodymium nitrate was added to the alcohol-water solution in the preparation of neodymium doped TiO_2 polymeric sol. The tubular membranes were coated by dip-coating method for 10 minutes for total saturation of the pore structure. The third modified MF membrane was prepared by using 20 wt.% zirconium (ZrO_2) doped polymeric TiO_2 sol. The predetermined amount of zirconium propoxide was mixed with the titanium isopropoxide for the preparation of the stabilized alkoxide solution and polymeric sol was coated by dip coating method for 10 min (Yaltrık 2017).

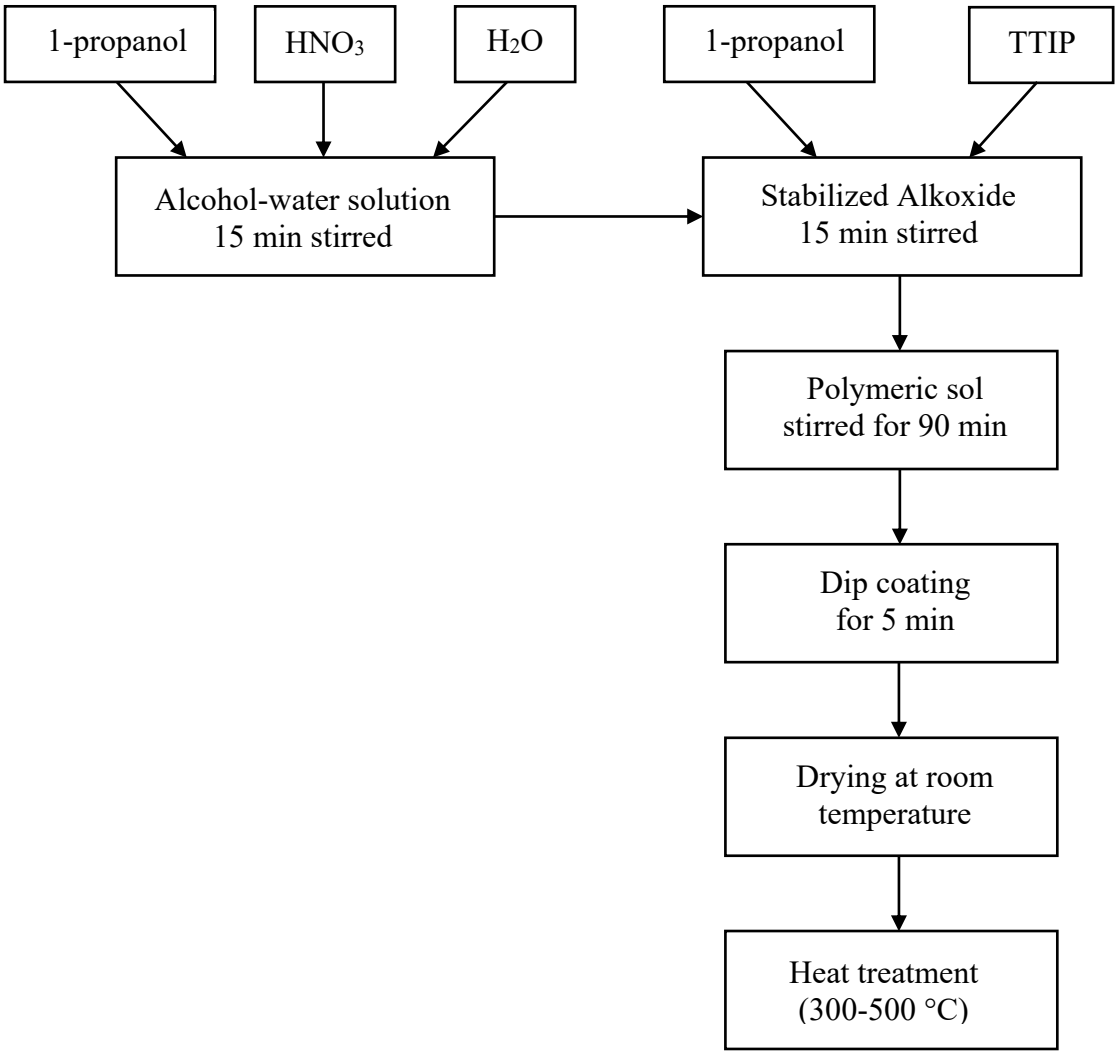

Figure 7.5. Flowchart of the modified MF layer preparation.

7.7. Preparation and Characterization of Emulsions

Emulsion was prepared by using edible oil, Tween-80 and distilled water. The oil content was set constant at 1 wt. % and an 8:1 weight ratio was used for the oil and surfactant ratio. Oil and surfactant were added to the water and mixed by using a blender for 2.5 min to generate a well-mixed and stable emulsion. Figure 7.6. shows preparation process of the emulsion. Blender was used at high speed and the emulsion was hold undisturbed for couple of hours to obtain foam-free emulsion before membrane treatment.

Prepared emulsions were characterized by Zetasizer NanoZS in order to determine the droplet size distribution in the oil-in-water emulsion. Olympus CH30/CH40 biological microscope was used to observe oil droplets and measure droplet size of emulsion. Total suspended solid and turbidity of feed and permeate streams were determined by Hach Lange DR 3900.

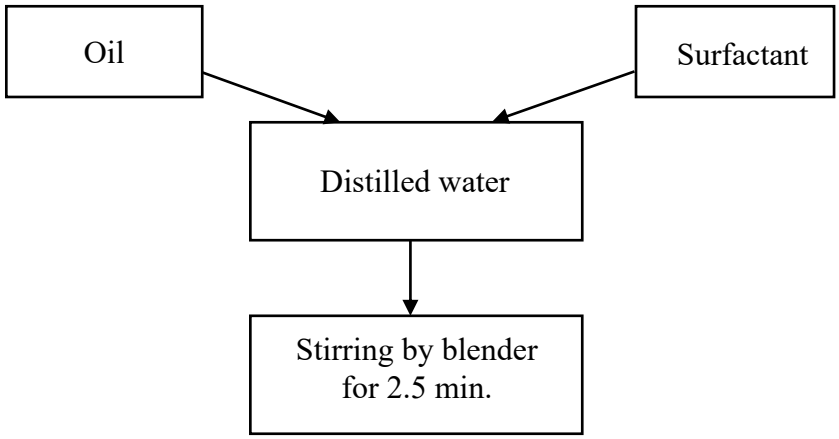

Figure 7.6. Flowchart of emulsion preparation.

7.8. Filtration Experiments

Filtration experiments were performed by a cross flow filtration system shown in Figure 7.7. Tubular membrane was placed into the stainless steel membrane module. Oily water was fed to the feed tank. CFV was changed from control panel as F notation. CFVs corresponding to each F value are listed in Table 7.2. Four different F values which were F= 10, F= 20, F= 30 and F= 35 were studied in this work. TMP was set from needle valve

and TMP was calculated by using gauge readings. 1 and 2 bar TMP were studied for oily water treatment. Permeate was collected for each treatment and flux was determined as a function of time based on the membrane surface area. Effect of temperature was investigated from room temperature to 40 °C. Temperature was controlled by using an immersion cooler.

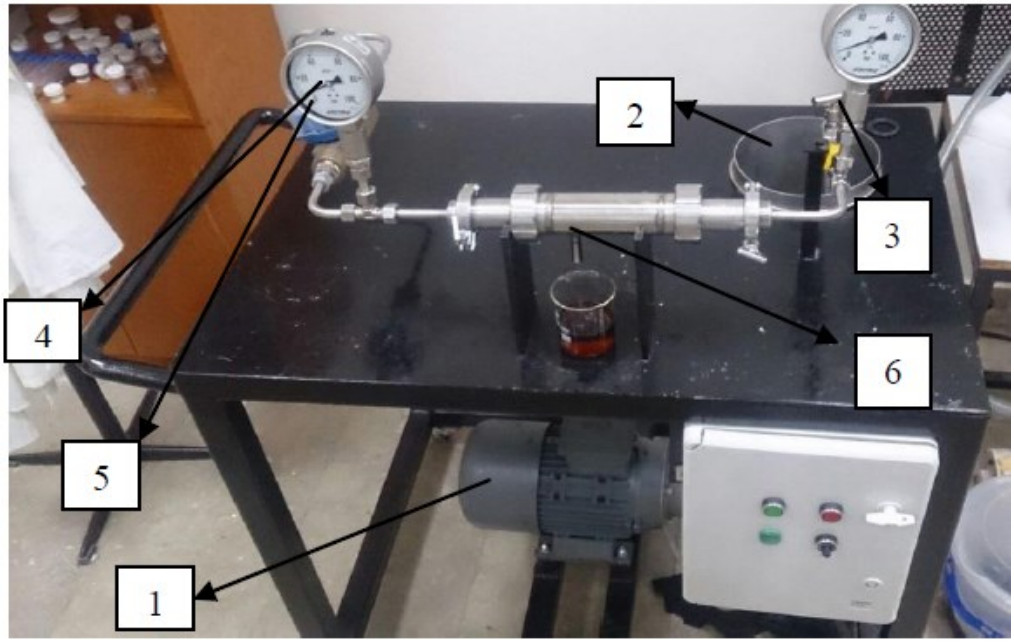

Figure 7.7. The filtration set-up (1-pump, 2-feed tank, 3- recycle, 4-gauge, 5-flowmeter, 6-cross-flow membrane module).

Table 7.2. CFV ranges corresponding to F values

F value	CFV (m/s)
5	0.15 - 0.20
10	0.30 - 0.35
15	0.40 - 0.45
20	0.45 - 0.50
25	0.55 - 0.65
30	0.70 - 0.80
35	0.90 – 1

CHAPTER 8

RESULTS AND DISCUSSION

8.1. Preparation of Support

Ceramic porous asymmetric supports were produced by extrusion of pastes which were prepared by using 5.2, 1.3 and 0.5 µm Al_2O_3 powders in size. Ceramic supports were produced in tubular shape with 16/25 mm inner/outer diameter and 200 mm in length. Tubular ceramic alumina supports are shown in Figure 8.1.

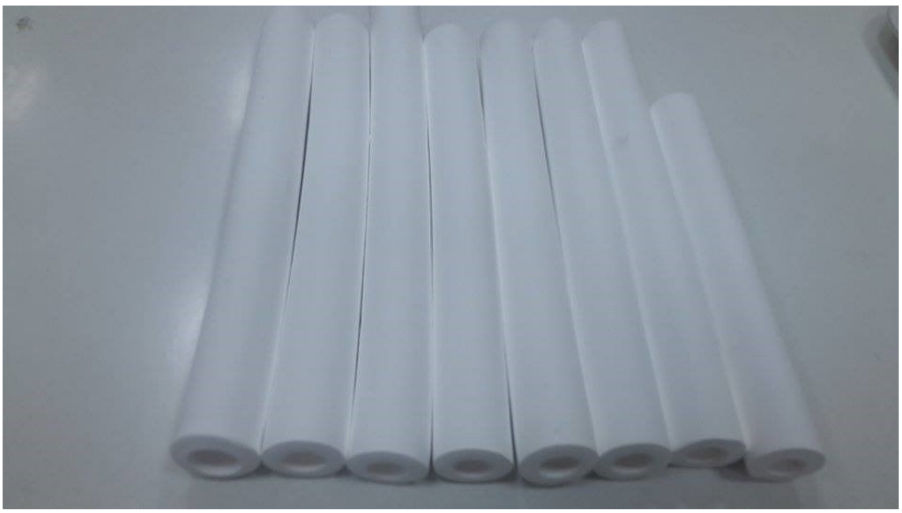

Figure 8.1. Tubular ceramic alumina supports.

8.2. Emulsion Characterization

Emulsions were prepared by edible oil, Tween-80 and distilled water with five different oil and surfactant weight ratios as 20:1, 14:1, 8:1, 4:1 and 2:1. Droplet size distributions of the emulsions with 20:1, 8:1 and 2:1 oil/surfactant weight ratios are given in Figures 8.2, 8.3 and 8.4. Peak particle sizes of the emulsions were about 5500 nm (5.5 µm) for all weight ratios. Some of the oil droplets were less than 1 µm in size. Oil droplets 0.6, 0.5 and 0.16 µm in size were observed when oil/surfactant weight ratio was 20:1 as seen in Figure 8.2.

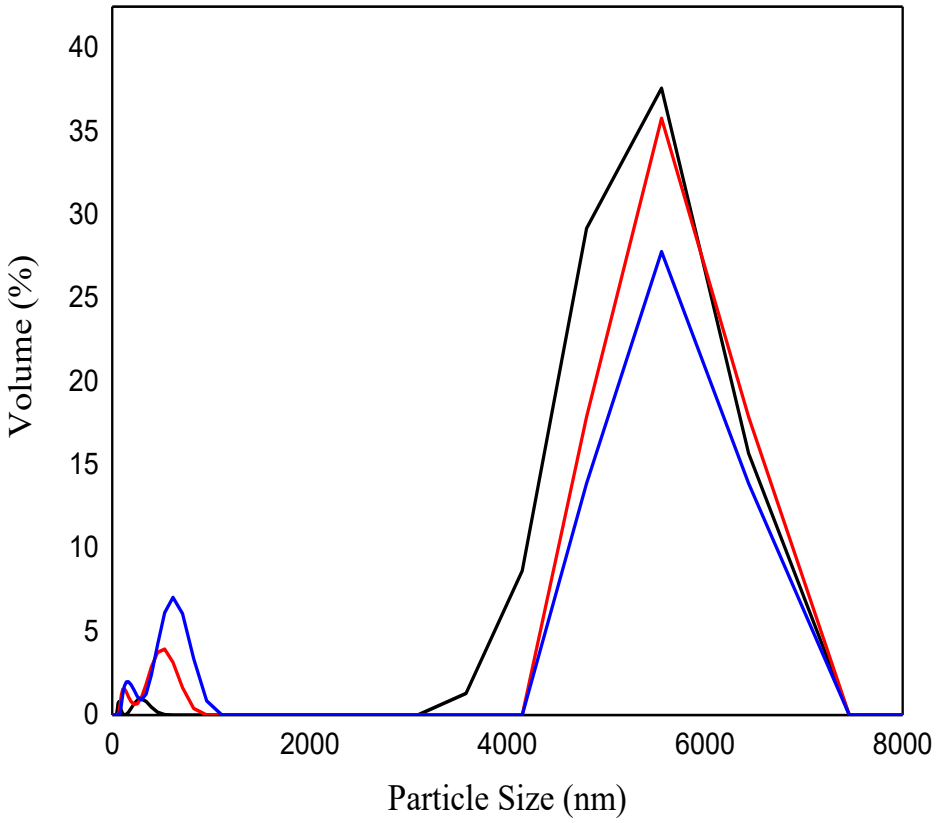

Figure 8.2. Droplet size distributions of the emulsion with 20:1 oil/surfactant weight ratio.

Oil/surfactant weight ratio was commonly used as 8:1 in the literature. The 8:1 ratio was used in this study since almost unimodal particle size distributions (almost no nanosized/submicron droplets) were observed for these 8:1 emulsions. A very small amount of the oil droplets were observed at 0.3 μm as seen in Figure 8.4. Emulsion with 2:1 weight ratio had the highest surfactant content. The presence of a bimodal particle size distribution (about 5.5 and 1 μm along with very small droplets) is more evident as seen in Figure 8.4. The emulsions prepared with 8:1 oil/surfactant ratio had the most uniform droplet size distributions and were used in the bulk of this thesis work.

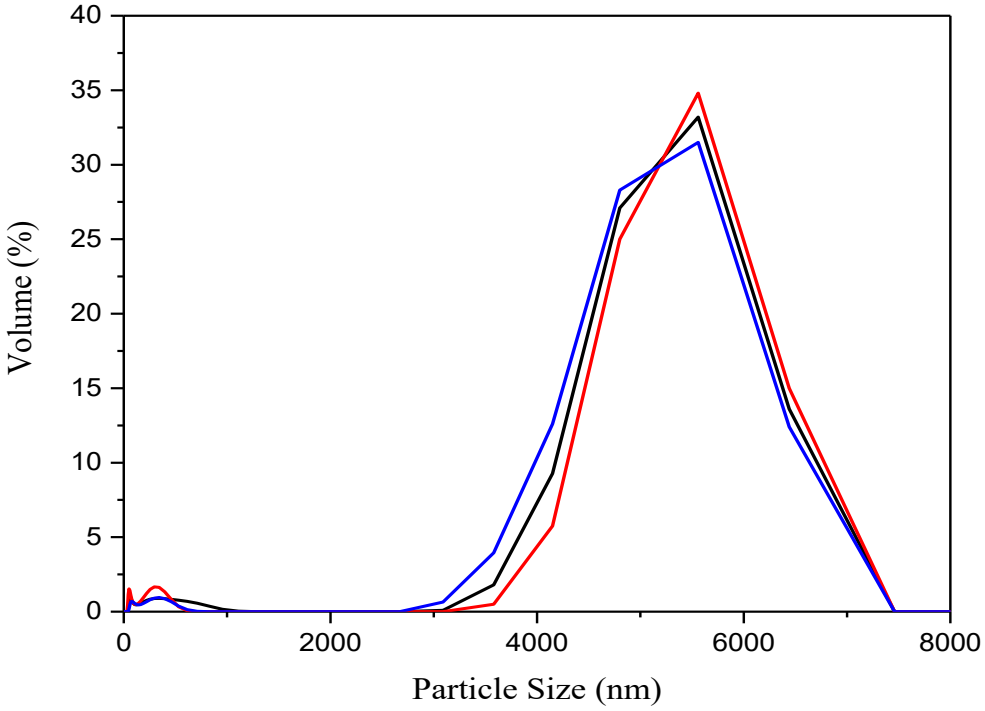

Figure 8.3. Droplet size distributions of the emulsion with 8:1 oil/surfactant weight ratio.

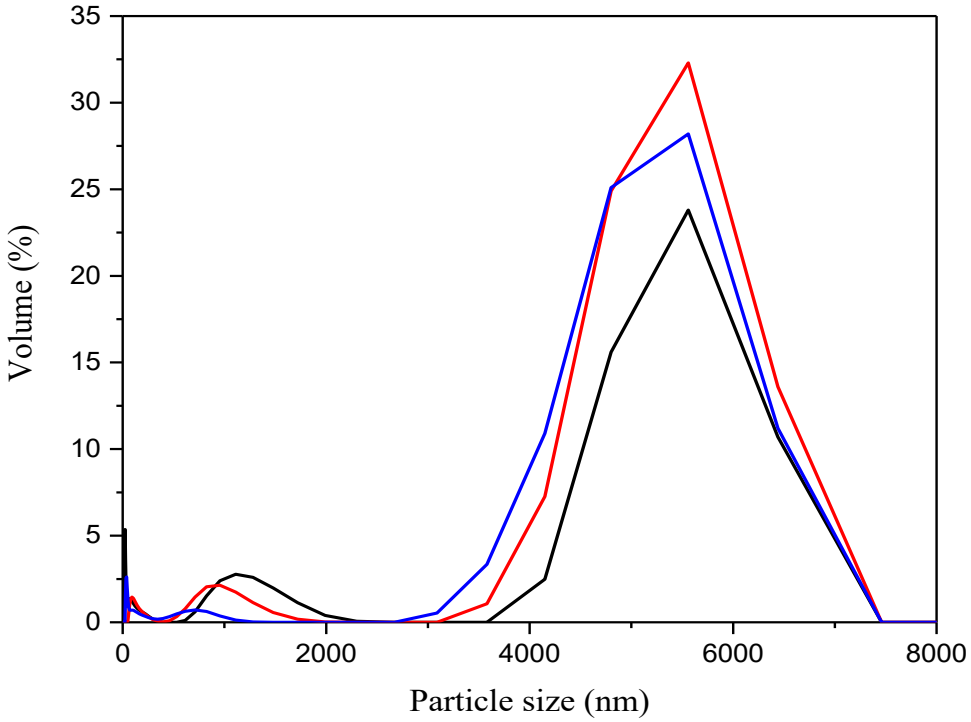

Figure 8.4. Droplet size distributions of the emulsion with 2:1 oil/surfactant weight ratio.

Droplet size distributions of the oil droplets which were determined by Zeta sizer were supported by biological microscope imaged obtained at different magnifications. The images obtained 10X magnification (Figure 8.5) have shown that oil droplets had a relatively bigger droplet size on the surface of the glass slide. Smaller oil droplets were observed at 40X magnification as can be seen in Figure 8.6. It was observed that the majority of the oil droplets had diameters in the 5.5 – 6 µm range. Smaller and bigger oil droplets were also observed. Smaller oil droplets which were almost 1 µm and less than 1 µm had been detected by Zeta sizer. Bigger oil droplets were most likely a consequence of the interaction of oil droplets in the emulsion placed on the microscope slide. Oil droplets attracted each other and formed bigger oil droplets quickly at the emulsion/air interface during the optical microscopy imaging. Continuous flow and movement of oil droplets were also observed on the emulsion surface on the microscope glass slide.

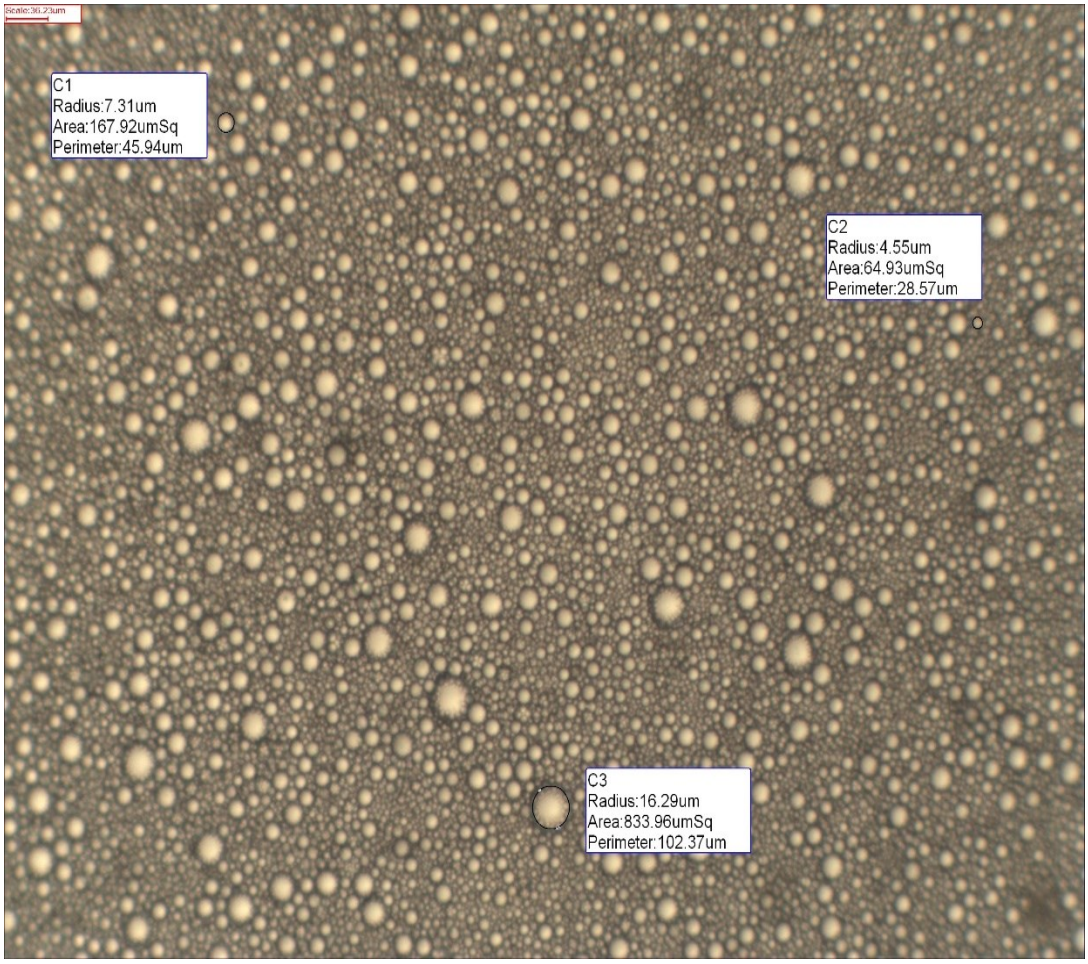

Figure 8.5. Microscope image of oil droplets with at 10X magnification.

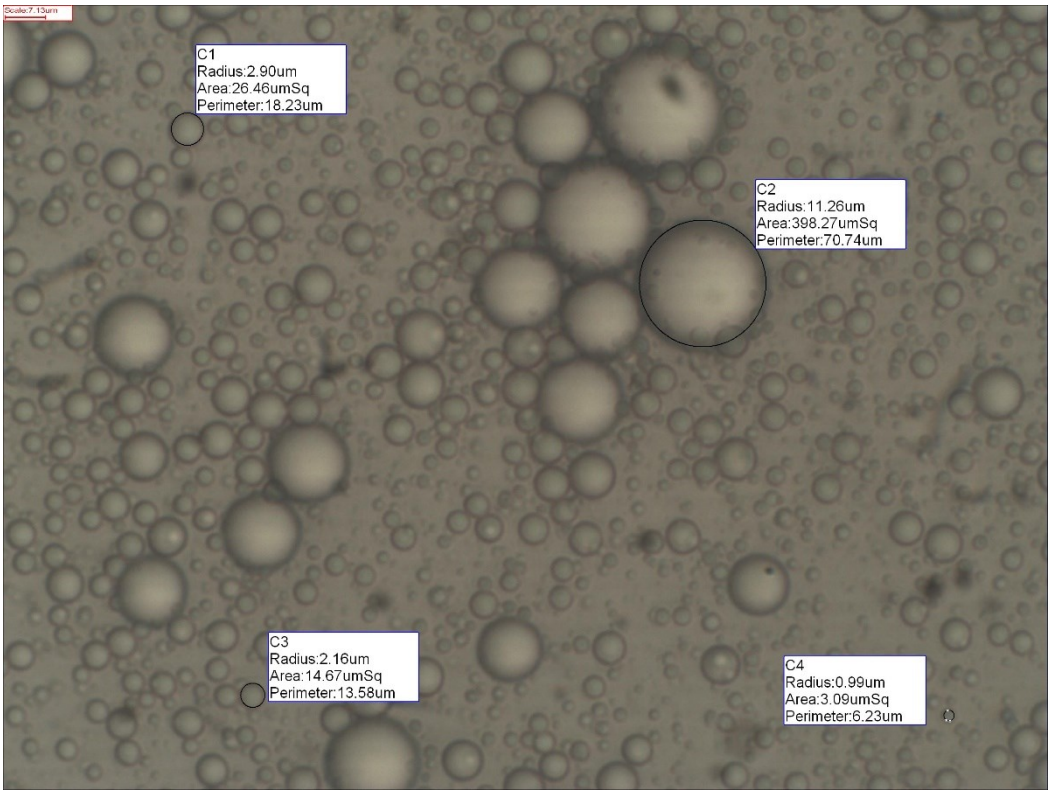

Figure 8.6. Microscope image of oil droplets at 40X magnification.

8.3. Determination of Emulsion Flux

Emulsions which were prepared by 8:1 weight ratio of oil and Tween-80 was fed to the membrane filtration system. Microfiltration, ultrafiltration and modified microfiltration membranes were used under different transmembrane pressures and crossflow velocities.

8.3.1. Emulsion Flux with Support

Three different supports were used to determine the time dependent change of permeate flux for both water and emulsion. The deionized water flux of Support 1 variation as a function of time is given in Figure 8.7. The permeates were collected for every five to ten minutes and the volumes were used for flux determination through the fixed membrane surface area. A relatively high and almost steady permeate flux were observed during the filtration experiment. The water flux variation with time for support 2 and support 3 are given in Figure 8.8. The initial Support 2 flux was about 2000 l/m^{2}h

but decreased very sharply to 315 l/m^{2}h. This very low permeate flux was attributed to the fouling/blockage of the membrane pore structure by gas bubbles on the support surface. Support 3 had a stable permeate flux at around 1500-1200 l/m^{2}h.

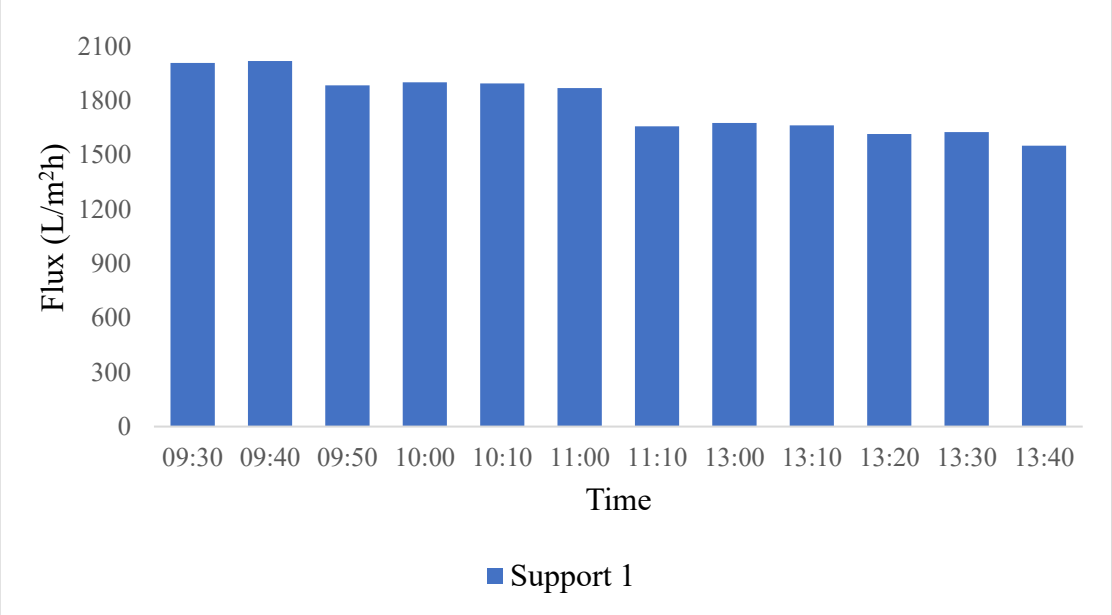

Figure 8.7. Pure water flux of the Support 1 for two days.

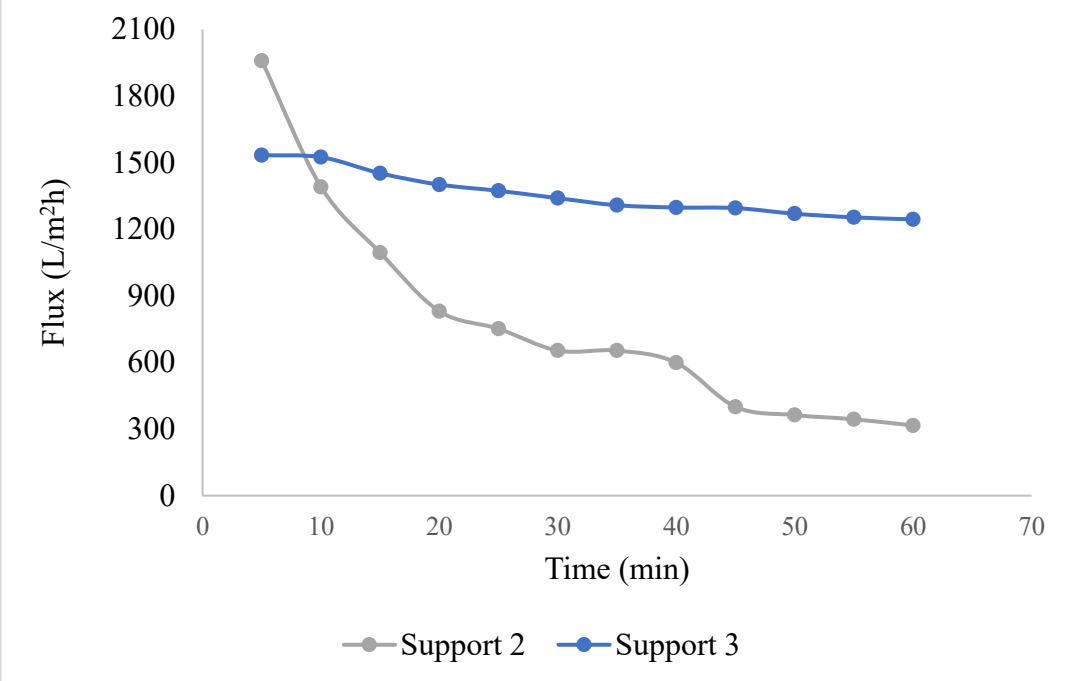

Figure 8.8. Pure water flux of Support 2 and Support 3.

First support had been used to determine pure water permeate flux so stable permeate flux of the emulsion was observed but it was not sufficient for the support. This support could be plugged with gas bubble during the determination of the pure water flux. Support 4 and Support 5 were clean so they had not been in order to determine pure water flux of the support. Permeate flux of these two supports suddenly decreased after 5 minutes later. Initial and final permeate fluxes of these supports were not reasonable because they were too low. The flux vs time variation for the supports with 1 wt.% of emulsion treatment is given in Figure 8.9.

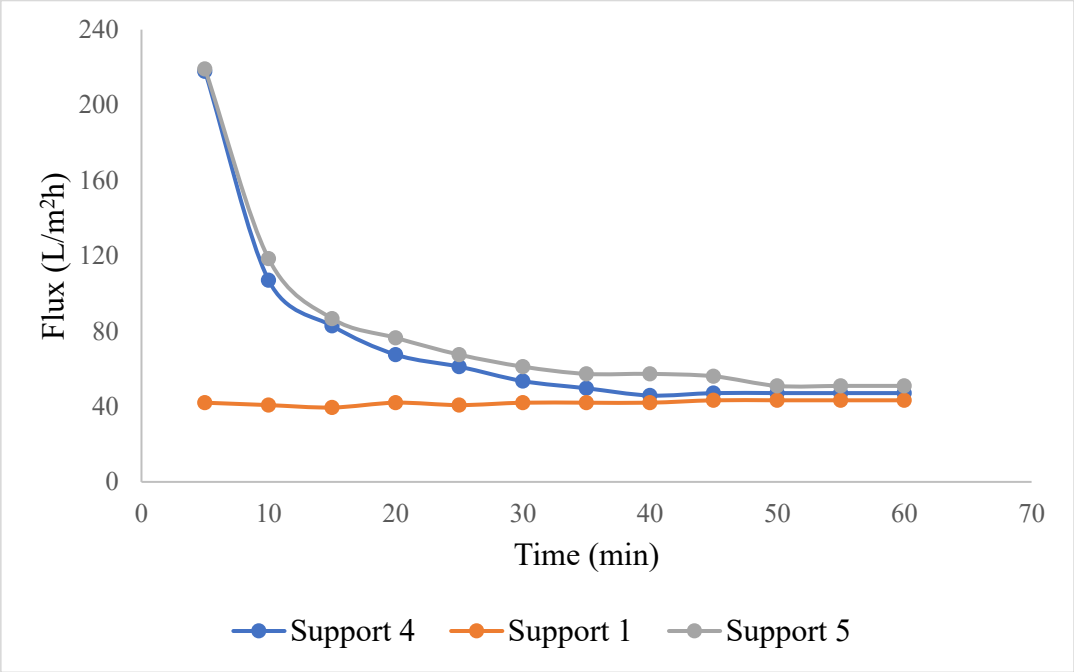

Figure 8.9. Permeate flux of Support 1, Support 4 and Support 5 with emulsion.

8.3.2. Emulsion Flux with Microfiltration

Effect of CFV was determined under three different F values (each F value on the control panel corresponds to a specific CFV range) which were 10, 20, 30 and 35. TMP was increased from 1 bar to 2 bar during the experiment in order to investigate effect of TMP on permeate flux. Figure 8.10. shows the pure water flux of the MF membrane. The highest pure water flux was observed as 500 l/m^{2}h at 2 bar of TMP with F=30 of CFV. Increasing CFV increased the emulsion permeate flux by decreasing membrane fouling

and concentration polarization. Figure 8.11. shows the effect of CFV on permeate flux at 1 bar of TMP. Increasing CFV may have increased turbulent flow and mass transfer coefficient. Membrane fouling was at its lowest level when F value was 35 (CFV was around 1 m/s). On the other hand, a significant flux decline was not observed for F=20 and F=30. However, initial flux decreased from 106 to 32 l/m^{2}h when F value was reduced from 35 to 20. Permeate flux of the emulsion increased with time when CFV was 1 m/s because temperature of the filtration system increased during the filtration. Figure 8.12. shows the effect of temperature on permeate flux. Results of the experiment showed that, temperature had a significant effect on permeate flux. Flux of the MF membrane increased from 106 to 129 l/m^{2}h when temperature was changed from 24 to 47 °C. Increasing temperature causes to low viscosity and decreasing viscosity causes turbulent flow. Therefore, flux increases because membrane surface is prevented from accumulation of oil droplets.

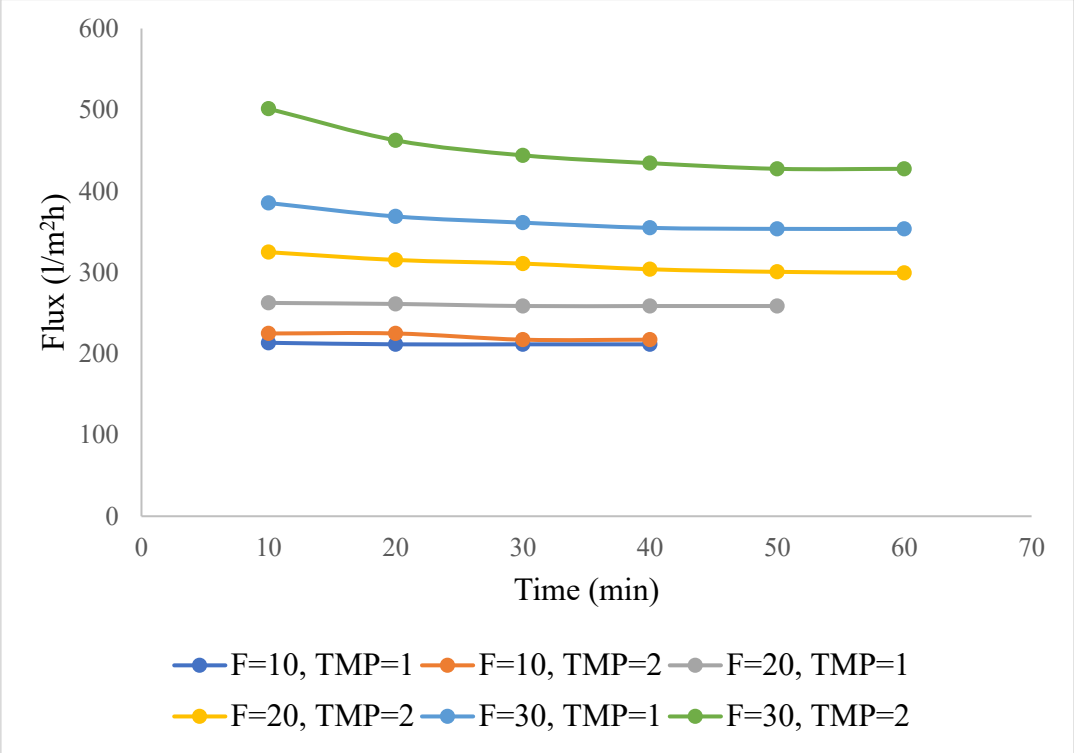

Figure 8.10. Effect of TMP and CFV on pure water flux of the MF membrane.

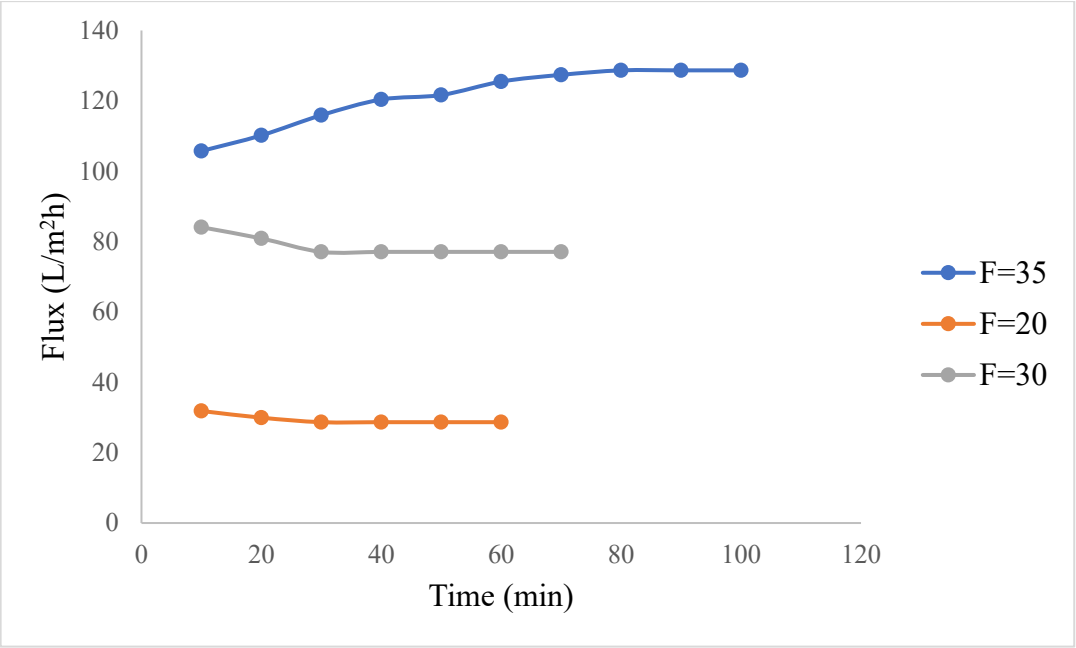

Figure 8.11. Effect of CFV on permeate flux of the MF membrane at 1 bar of TMP.

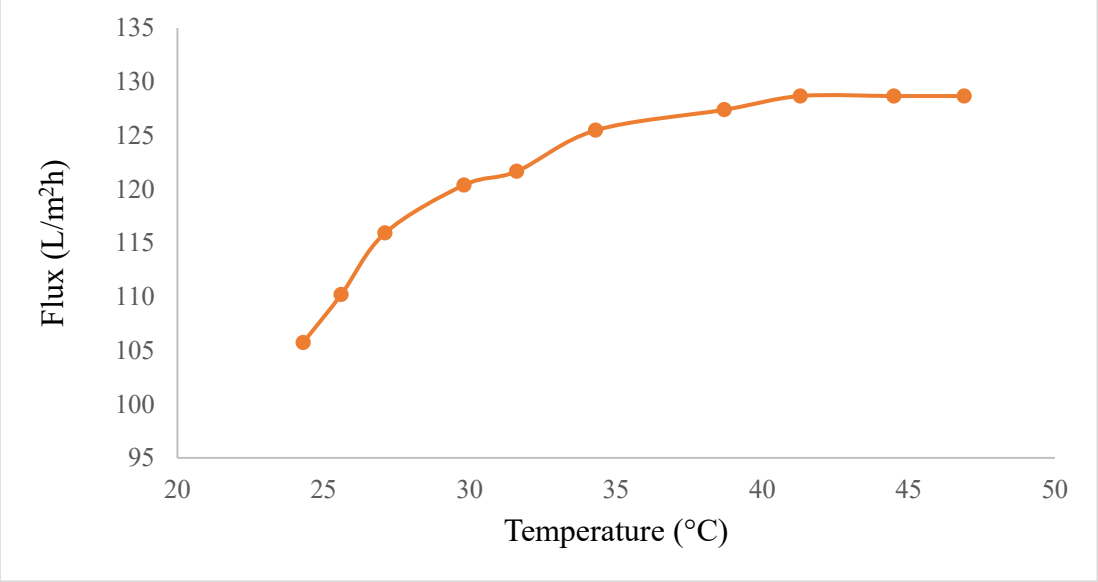

Figure 8.12. Effect of temperature on permeate flux of the MF membrane (TMP: 1 bar F=35).

Experiment was performed at 2 bar of TMP. Permeate flux at 2 bar of TMP was more stable than 1 bar for the same F values. Temperature of the membrane filtration system was around 47 °C. Flux decline was not observed due to high temperature as shown in Figure 8.13. However, decreasing CFV caused low permeate flux at 1 bar of

TMP. Increasing TMP from 1 to 2 bar enhanced permeate flux for all CFVs as in Figure 8.14. However, there was no significant effect when flow was low. Steady and high permeate flux was obtained at 2 bar of TMP with 1 m/s of CFV.

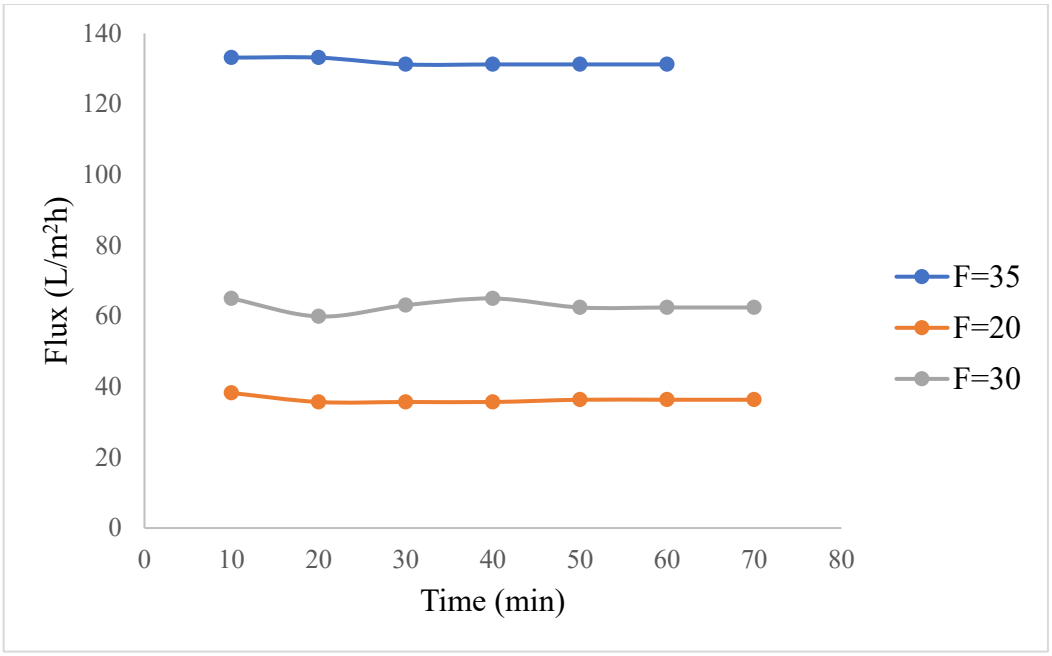

Figure 8.13. Effect of CFV on permeate flux of the MF membrane at 2 bar of TMP.

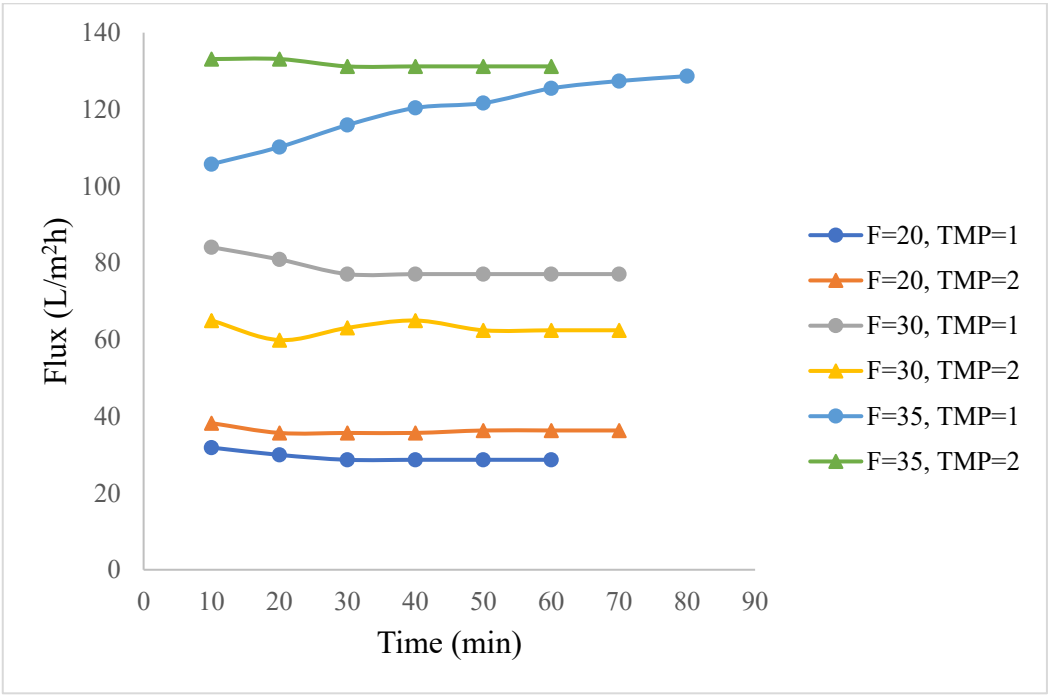

Figure 8.14. Effect of TMP and CFV on emulsion permeate flux of the MF membrane.

8.3.3. Emulsion Flux with Ultrafiltration

Effect of CFV and TMP were investigated by ultrafiltration membrane (Microfiltration + Disperal + two times of P2 coating). 1 wt. % emulsion was used for the filtration. Three different F values were set on the control panel as 10, 20 and 30. When F value was 10 (approximately 0.30 m/s), steady flux was obtained with 9 l/m^{2}h at 1 bar of TMP as shown in Figure 8.15. Initial permeate flux was increased to 33 l/m^{2}h with increasing CFV as 0.50 m/s (F=20) but flux decreased to 22 l/m^{2}h during the filtration because of membrane fouling. Flux increased with time when CFV was increased to F=30 and flux increased with time. Fouling layer has not yet formed a second layer and increasing CFV removed oil droplets on the membrane surface. Steady permeate flux was achieved when TMP was 2 bar as shown in Figure 8.16. There was no significant flux decline and membrane fouling. 53 l/m^{2}h of permeate flux was obtained by F=30. TMP had a significant effect on permeate flux.

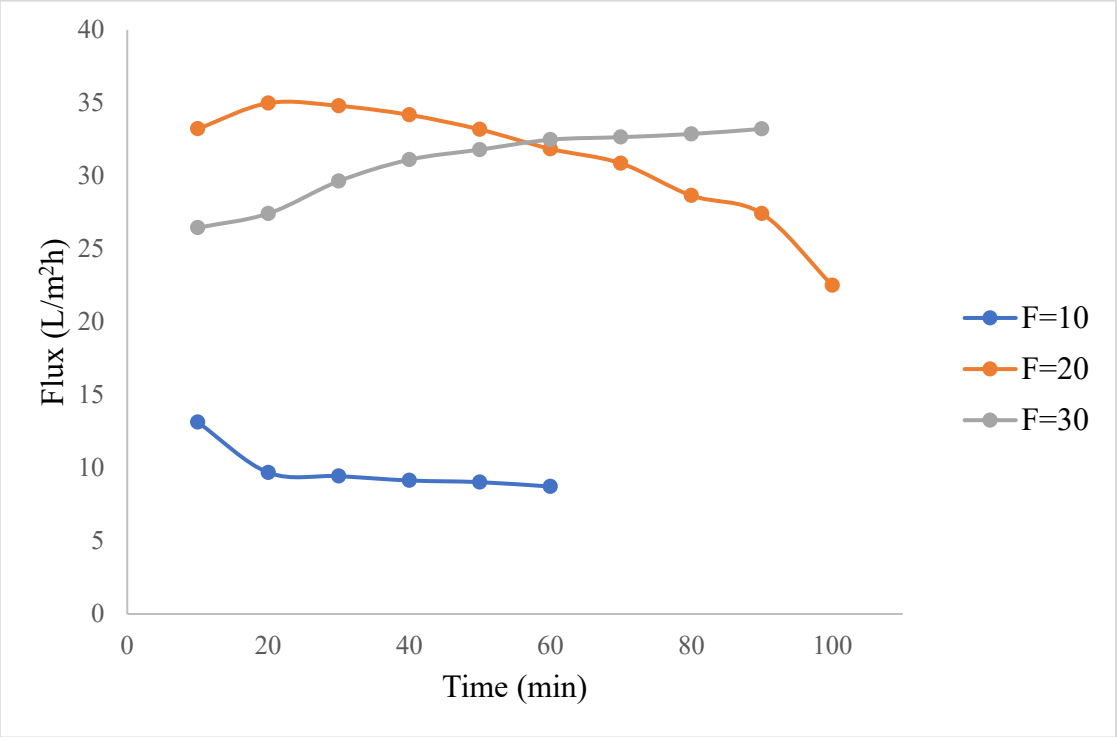

Figure 8.15. Effect of CFV on permeate flux of the UF membrane at 1 bar of TMP.

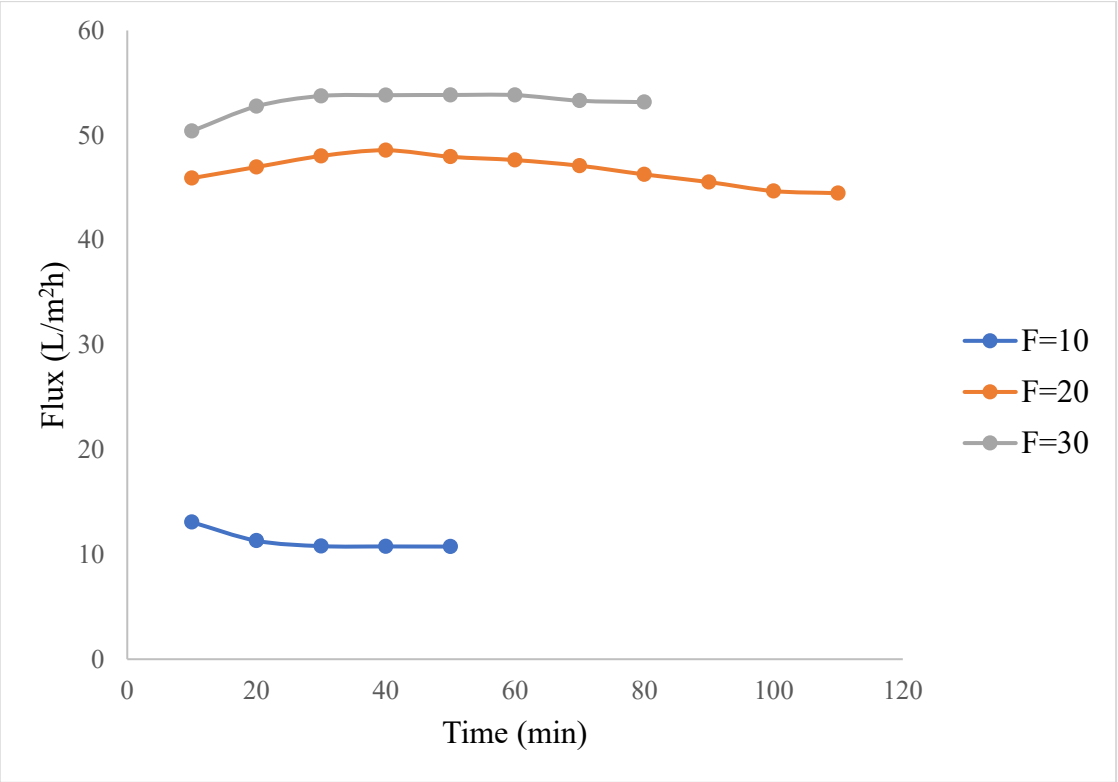

Figure 8.16. Effect of CFV on permeate flux of the UF membrane at 2 bar of TMP.

8.3.4. Emulsion Flux with Modified MF Membranes

Three different modified MF membranes which were MF + 1 wt.% pure TiO_2, MF + Nd doped (5 wt.%) TiO_2 and MF + ZrO_2 doped (20 wt.%) TiO_2 were used to determine permeate flux at 2 bar and F=30 CFV. MF + ZrO_2 doped (20 wt.%) TiO_2 had the lowest permeate flux but MF + 1 % pure titania and MF + Nd doped (5 wt.%) TiO_2 were very close to each other. It was expected that, modified membranes should have had higher permeate flux according to literature. Modification of the layers may not have been correctly prepared and coated. Figure 8.17. shows emulsion flux of the modified MF membranes.

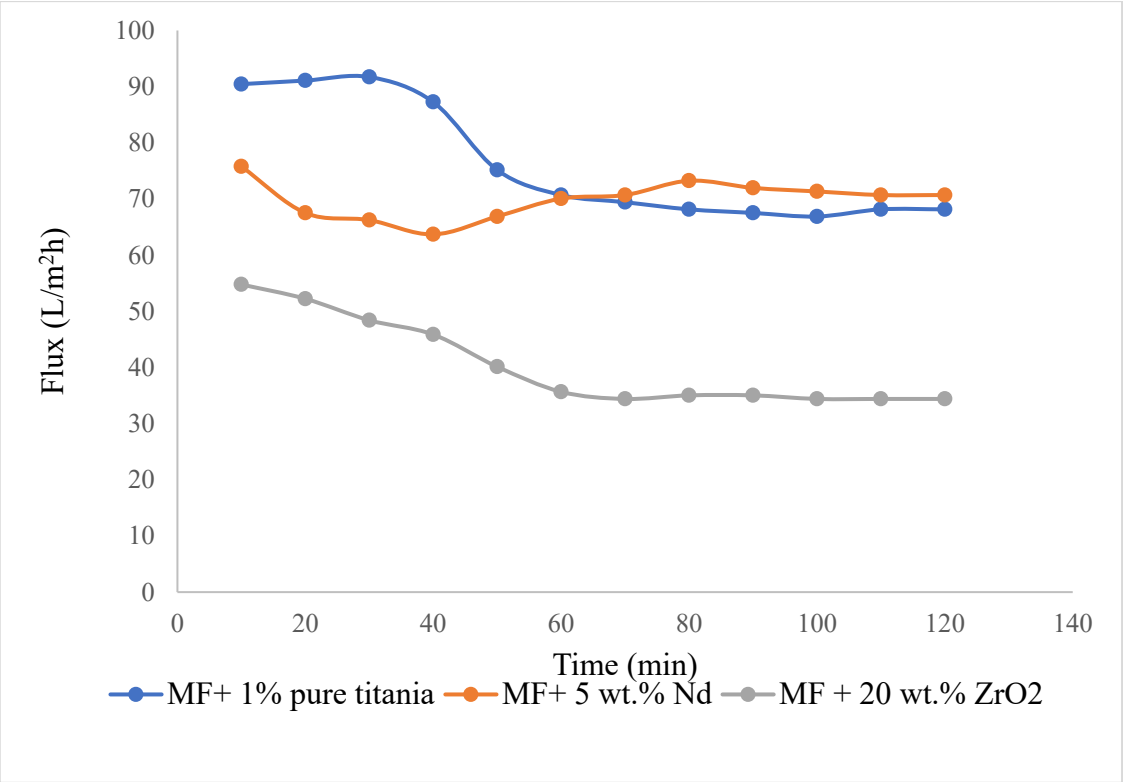

Figure 8.17. Determination of Modified MF membranes flux at 2 bar of TMF with F= 30 CFV.

8.4. Permeate Characterization

Calibration curve was obtained from turbidity values of initial 1 wt. % of the emulsion in order to understand the removal efficiency of the membranes. Figure 8.18. shows the calibration curve. Turbidity and total suspended solid were determined in order to characterize initial emulsion and permeate. Table 8.1. shows the turbidity and TSS of feed and permeate for all membranes. Over than 99.71% and 99.80 % of the removal efficiency of TSS and turbidity were achieved for all membranes. Final feed concentration of the all membranes reached discharge criteria except support 4 and support 5. Supports were not useful to reach discharge criteria. The color changes of emulsions after the filtration treatment by using support and MF membranes are shown in the pictures given in Figures 8.19. and 8.20. The emulsion was completely cleaned and totally transparent permeate was obtained for all membranes but supports could not provide requirements.

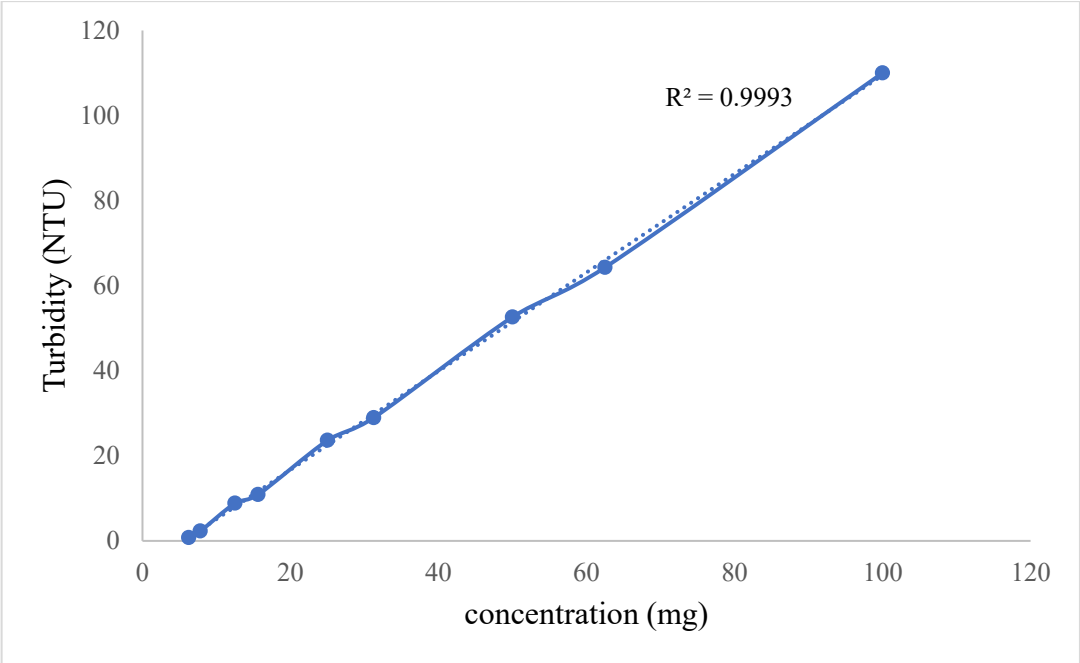

Figure 8.18. Calibration curve of the 1 wt. % emulsion in terms of turbidity.

Table 8.1. Characterization of feed and permeate.

			Retention (%)	
	Turbidity value	**Permeate concentration (mg/l)**	**TSS**	**Turbidity**
Support 1	0	6.09	99.94	100
Support 4	15.9	20.47	99.71	99.80
Support 5	14.3	19.05	99.74	99.82
MF	0	0	100	100
UF	0	0	100	100
MF+ 1 wt.% pure titania	0	1.52	100	100
MF+5 wt.% Nd	0	1.28	100	100
MF+20 wt.% ZrO_2	0	0	100	100

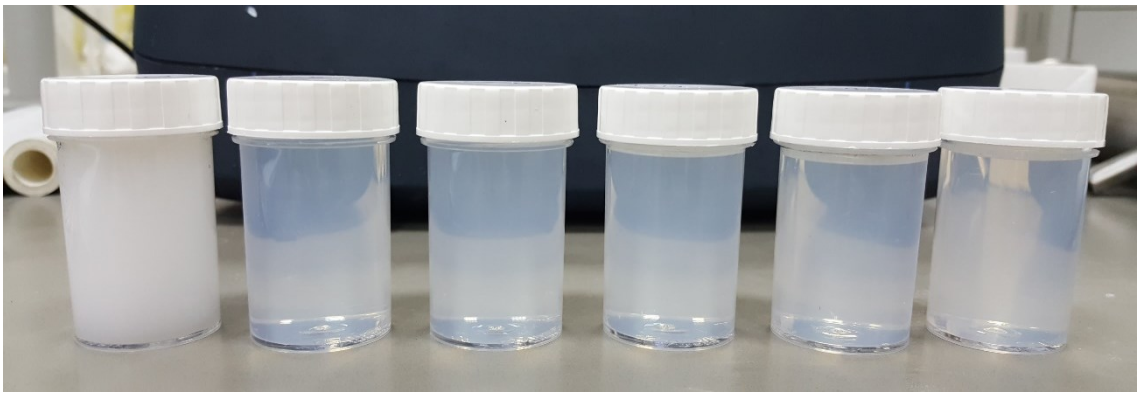

Figure 8.19. Color change of emulsion after filtration experiment with support.

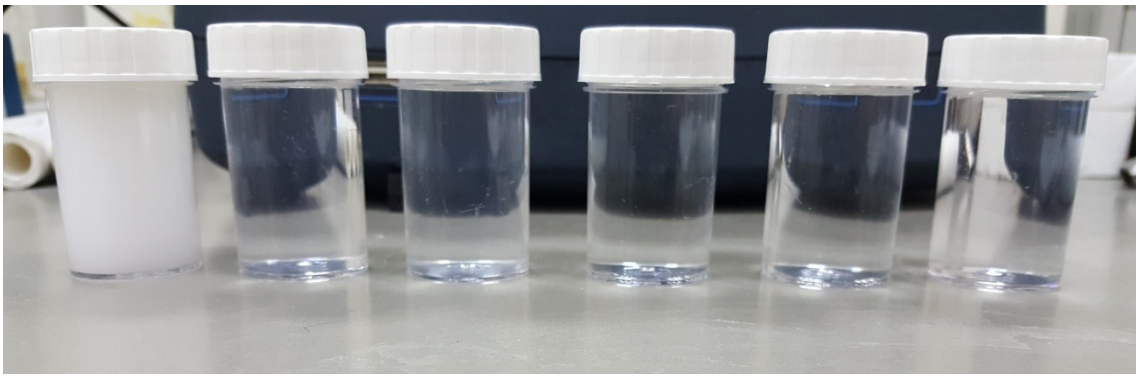

Figure 8.20. Color change of emulsion after filtration experiment with MF.

CHAPTER 9

CONCLUSIONS

Tubular ceramic supports were produced by α- Al_2O_3 powder by extrusion method. Heat treated ceramic supports were coated with α- Al_2O_3 MF sols by dip coating method. Two different types of UF layers were prepared by disperal and P2 powders. Heat treatment was applied for each MF and UF layers at 1200 °C and 600 °C, respectively. MF layer was coated with titania, zirconia and neodymium doped titania polymeric sols to enhance permeate flux without changing separation ability and characteristic of the MF layer by reducing interaction between oil droplets and membrane surface. Hydrophilicity of the membrane surface was changed by nano-coated polymeric sols. The CFV, TMP and temperature values were varied in the experimental work in order to understand their effects on obtaining high permeate fluxes. Different oil/surfactant weight ratios were used to obtain stable oil-in-water emulsions. The 8:1 ratio was the optimum ratio since almost unimodal particle size distributions were observed for these 8:1 emulsions.

Emulsion droplet size distributions were determined by Zeta sizer. Crossflow filtration set up was used to determine the performance of ceramic MF, UF and modified membranes. Spectrophotometer was used to analyze total suspended solids and turbidity.

Average droplet size of the emulsions was measured as 5.6 μm. Small portion of the oil droplets were less than 1 μm. Oil droplets were observed by an optical microscope with different magnification devices. Image of the oil droplets supported to the Zeta sizer results. Smaller oil droplets were observed with 40 times of magnification. CFV was changed from 0.30 to 1 m/s and two different transmembrane pressures were used as 1 and 2 bar for MF membrane. The highest pure flux was observed as 500 l/m^2h at 2 bar of TMP and 1 m/s of CFV for MF. The highest emulsion flux was obtained as 133 l/m^2h with the same conditions. Increasing CFV and TMP enhanced initial permeate flux of water and emulsion flux. When TMP was increased from 1 bar to 2 bar, initial permeate flux was increased from 105 l/m^2h to 133 l/m^2h for 1m/s of CFV. Stable permeate flux was observed with 2 bar of. Temperature increased from 24.3 to 46.9 °C during the experiment and permeate flux enhanced from 106 to 129 l/m^2h. Increasing temperature

was a significant effect to obtain high permeate flux. Permeate flux of the UF membrane (MF + disperal + 2 times of P2) was less than MF membrane as expected. CFV was changed from 0.30 m/s to 0.80 m/s and steady permeate flux was achieved by 2 bar of TMP with 13, 46 and 50 l/m^2h of initial fluxes, respectively. Three different modified MF membranes which were MF + 1 wt.% pure TiO_2, MF + Nd doped (5 wt.%) TiO_2 and MF + ZrO_2 doped (20 wt.%) TiO_2 were used at 2 bar and F=30 CFV. The highest permeate flux was around 90 l/m^2h with MF + 1 wt.% pure TiO_2. Flux of the modified membranes were lower than MF membranes but modified membranes should have had higher permeate flux than MF membrane. TSS and turbidity of the emulsion were reduced as 100 % with MF and UF membranes. Final oil concentration of the permeate streams fulfill the discharge criteria.

In conclusion, MF and UF coated α- Al_2O_3 ceramic membranes were effective to remove oil from the water. CFV, TMP and temperature had a significant effect to enhance permeate flux. Concentration polarization and membrane fouling of the membrane surfaces can be controlled/minimized by an optimum CFV, TMP and temperature combination.

REFERENCES

Abadi, Sareh Rezaei Hosein, Mohammad Reza Sebzari, Mahmood Hemati, Fatemeh Rekabdar, and Toraj Mohammadi. 2011. "Ceramic membrane performance in microfiltration of oily wastewater." *Desalination* 265 (1):222-228. doi: https://doi.org/10.1016/j.desal.2010.07.055.

Baker, Richard W. 2012. *Membrane Technology and Applications*. New York, UNKNOWN: John Wiley & Sons, Incorporated.

Benito, J. M., A. Cambiella, A. Lobo, G. Gutiérrez, J. Coca, and C. Pazos. 2010. "Formulation, characterization and treatment of metalworking oil-in-water emulsions." *Clean Technologies and Environmental Policy* 12 (1):31-41. doi: 10.1007/s10098-009-0219-2.

Buekenhoudt, Anita. 2008. "Stability of Porous Ceramic Membranes." In *Membrane Science and Technology*, edited by Reyes Mallada and Miguel Menéndez, 1-31. Elsevier.

Burggraaf, A.J. 1996. "Important Characteristics of Inorganic Membranes." In *Fundamentals of inorganic membrane science and technology*, edited by A. J. Burggraaf and L. Cot, 21-34.

Chang, Qibing, Jian-er Zhou, Yongqing Wang, Jian Liang, Xiaozhen Zhang, Sophie Cerneaux, Xia Wang, Zhiwen Zhu, and Yingchao Dong. 2014. "Application of ceramic microfiltration membrane modified by nano-TiO2 coating in separation of a stable oil-in-water emulsion." *Journal of Membrane Science* 456 (Supplement C):128-133. doi: https://doi.org/10.1016/j.memsci.2014.01.029.

Chang, Qibing, Jian-er Zhou, Yongqing Wang, Jinming Wang, and Guangyao Meng. 2010. "Hydrophilic modification of Al2O3 microfiltration membrane with nano-sized γ-Al2O3 coating." *Desalination* 262 (1):110-114. doi: https://doi.org/10.1016/j.desal.2010.05.055.

Cheryan, M., and N. Rajagopalan. 1998. "Membrane processing of oily streams. Wastewater treatment and waste reduction." *Journal of Membrane Science* 151 (1):13-28. doi: https://doi.org/10.1016/S0376-7388(98)00190-2.

Coca, José, Gemma Gutiérrez, and José Manuel Benito. 2011. "Treatment of Oily wastewater." In *Water Purification and Management*, edited by José Coca-Prados and Gemma Gutiérrez-Cervelló, 1-55. Dordrecht: Springer Netherlands.

Eslamian, Saeid. 2016. *Urban Water Reuse Handbook*. Boca Raton: CRC Press. Book.

Gupta, Raju Kumar, Gary J. Dunderdale, Matt W. England, and Atsushi Hozumi. 2017. "Oil/water separation techniques: a review of recent progresses and future directions." *Journal of Materials Chemistry A* 5 (31):16025-16058. doi: 10.1039/C7TA02070H.

Hsieh, H. P. 1996a. "Historical development and commercialization of inorganic membranes." In *Membrane Science and Technology*, edited by H. P. Hsieh, 15-22. Elsevier.

Hsieh, H. P. 1996b. "Membranes and membrane processes." In *Membrane Science and Technology*, edited by H. P. Hsieh, 1-13. Elsevier.

Hua, F. L., Y. F. Tsang, Y. J. Wang, S. Y. Chan, H. Chua, and S. N. Sin. 2007. "Performance study of ceramic microfiltration membrane for oily wastewater treatment." *Chemical Engineering Journal* 128 (2):169-175. doi: http://dx.doi.org/10.1016/j.cej.2006.10.017.

Kajitvichyanukul, Puangrat, Yung-Tse Hung, and Lawrence K. Wang. 2011. "Membrane Technologies for Oil–Water Separation." In *Membrane and Desalination Technologies*, edited by Lawrence K. Wang, Jiaping Paul Chen, Yung-Tse Hung and Nazih K. Shammas, 639-668. Totowa, NJ: Humana Press.

Križan Milić, Janja, Arnela Murić, Irena Petrinić, and Marjana Simonič. 2013. "Recent Developments in Membrane Treatment of Spent Cutting-Oils: A Review." *Industrial & Engineering Chemistry Research* 52 (23):7603-7616. doi: 10.1021/ie4003552.

Lee, K.P. 2013. "Fabrication and Application of Nanoporous Alumina Membranes." Doctoral thesis Theses, Chemical Engineering, University of Bath.

Lee, Shi-Hee, Koo-Chun Chung, Min-Chul Shin, Jong-In Dong, Hee-Soo Lee, and Keun Ho Auh. 2002. "Preparation of ceramic membrane and application to the crossflow microfiltration of soluble waste oil." *Materials Letters* 52 (4):266-271. doi: https://doi.org/10.1016/S0167-577X(01)00405-0.

Levanen, Erkki. 2004. "Alumina Membranes- Colloidal Processing and Evolution of Functional Properties." Doctoral thesis Thesis, Tampere University of Technology.

Lobo, Alberto, Ángel Cambiella, José Manuel Benito, Carmen Pazos, and José Coca. 2006. "Ultrafiltration of oil-in-water emulsions with ceramic membranes: Influence of pH and crossflow velocity." *Journal of Membrane Science* 278 (1):328-334. doi: http://dx.doi.org/10.1016/j.memsci.2005.11.016.

Lu, Dongwei, Tao Zhang, Leo Gutierrez, Jun Ma, and Jean-Philippe Croué. 2016. "Influence of Surface Properties of Filtration-Layer Metal Oxide on Ceramic Membrane Fouling during Ultrafiltration of Oil/Water Emulsion." *Environmental Science & Technology* 50 (9):4668-4674. doi: 10.1021/acs.est.5b04151.

Nair, Lakshmy M., Norma V. Stephens, Sarah Vincent, Neervalur Raghavan, and Patrick J. Sand. 2003. "Determination of polysorbate 80 in parenteral formulations by high-performance liquid chromatography and evaporative light scattering detection." *Journal of Chromatography A* 1012 (1):81-86. doi: https://doi.org/10.1016/S0021-9673(03)01105-1.

Padaki, M., R. Surya Murali, M. S. Abdullah, N. Misdan, A. Moslehyani, M. A. Kassim, N. Hilal, and A. F. Ismail. 2015. "Membrane technology enhancement in oil–water separation. A review." *Desalination* 357 (Supplement C):197-207. doi: https://doi.org/10.1016/j.desal.2014.11.023.

Rijn, C. J. M. van. 2004. "Overview membrane technology." In *Membrane Science and Technology*, edited by C. J. M. van Rijn, 1-23. Elsevier.

Salahi, Abdolhamid, Mohsen Abbasi, and Toraj Mohammadi. 2010. "Permeate flux decline during UF of oily wastewater: Experimental and modeling." *Desalination* 251 (1):153-160. doi: https://doi.org/10.1016/j.desal.2009.08.006.

Šereš, Zita, Nikola Maravić, Aleksandar Takači, Ivana Nikolić, Dragana Šoronja-Simović, Aleksandar Jokić, and Cecilia Hodur. 2016. "Treatment of vegetable oil refinery wastewater using alumina ceramic membrane: optimization using response surface methodology." *Journal of Cleaner Production* 112 (Part 4):3132-3137. doi: https://doi.org/10.1016/j.jclepro.2015.10.070.

Srijaroonrat, P., E. Julien, and Y. Aurelle. 1999. "Unstable secondary oil/water emulsion treatment using ultrafiltration: fouling control by backflushing." *Journal of Membrane Science* 159 (1):11-20. doi: http://dx.doi.org/10.1016/S0376-7388(99)00044-7.

Tsuru, T. 2008. "Nano/subnano-tuning of porous ceramic membranes for molecular separation." *Journal of Sol-Gel Science and Technology* 46 (3):349-361. doi: 10.1007/s10971-008-1712-5.

Tsuru, Toshinori, Takashi Sudoh, Tomohisa Yoshioka, and Masashi Asaeda. 2001. "Nanofiltration in non-aqueous solutions by porous silica–zirconia membranes." *Journal of Membrane Science* 185 (2):253-261. doi: https://doi.org/10.1016/S0376-7388(00)00651-7.

Yaltrık, Kaan. 2017. "Preparation and Application of Subnano Ceramic Filtration Membranes for Organic Species Removal from Aqueous Streams." Chemical Engineering, İzmir Institute of Technology.

Yılmaz, Kenan. 2016. "Rheological Characterization and Extrusion of Alumina Based Pastes for The Preparation of Tubular Ceramic Membrane Supports." İzmir Institute of Technology.

Yu, Li, Mei Han, and Fang He. 2013a. "A review of treating oily wastewater." *Arabian Journal of Chemistry* 10 (Supplement 2):S1913-S1922. doi: https://doi.org/10.1016/j.arabjc.2013.07.020.

Yu, Li, Mei Han, and Fang He. 2013b. "A review of treating oily wastewater." *Arabian Journal of Chemistry* 10:S1913-S1922. doi: http://dx.doi.org/10.1016/j.arabjc.2013.07.020.

Zhou, Jian-er, Qibing Chang, Yongqing Wang, Jinming Wang, and Guangyao Meng. 2010. "Separation of stable oil–water emulsion by the hydrophilic nano-sized ZrO2 modified Al2O3 microfiltration membrane." *Separation and Purification Technology* 75 (3):243-248. doi: https://doi.org/10.1016/j.seppur.2010.08.008.